UNIVERSITY of HOUSTON

EXPERIMENTAL STUDY OF JAPAN LIFE'S FINE CERAMICS INSERT (FCI)

Submitted to:

Japan Life Co., Ltd.
Tokyo, Japan

Prepared by:

Abdeldjelil Belarbi, Ph.D., PE, Distinguished Professor
&
Abdelmounaim Mechaala, Ph.D. Post Doctoral Fellow
Department of Civil and Environmental Engineering
University of Houston

July 6, 2023

TABLE OF CONTENTS

1 Introduction

To connect structural elements with each other or to fix non-structural components and systems to reinforced concrete structures, different types of anchors can be used with different mounting systems. These anchor types can be divided broadly into two categories: post-installed and cast-in anchors, where each anchor type has different performance specifications and failure modes. The cast-in anchors are installed in place prior to concrete (e.g., headed bolts, headed studs, and hooked bolts), while the post-installed anchors are installed inside a pre-drilled hole (e.g., expansion and undercut). The selection of the specific anchor type is based on the requirements of the project.

Some research has been carried out to understand the behavior of the anchors according to how they are mounted in reinforced concrete structures and the load they carry. In addition, the anchor characteristics and concrete properties have a major impact in determining the failure modes that can occur when the anchored systems are loaded (e.g., concrete breakout, steel failure, concrete splitting, bond failure, etc.), which can lead to the detachment of the fastened item and cause structural damage. To avoid such failures, having accurate prediction models and design equations of the anchor capacity under different load loading conditions (tension, shear, combination of tension/shear, and combination of shear/moment) is, therefore, important. Furthermore, the anchors can experience different modes of loading such as monotonic, cyclic, fatigue, and sustained loading, the effect of which is also important to predict with reagrds to anchor capacity and failure mode.

Numerous studies have dealt with rupture modes under load-displacement behavior (Fuchs et al. 1995, Elgehausen and Balogh 1995 Cook e al. 1998, Ghobarag et al. 2004 Eligehausen et al., 2006, Al-Taan et al. 2012, Jin-Sup et al. 2013, etc.). In more recent investigations, and by way of example but not all-inclusive, many researchers have investigated systems with different failure modes of the post-installed anchors for both bonded and mechanical anchor types (Sharnouby and Naggar, 2010, Jin-Sup et al. 2013, Delhomme et al. 2018, Mahrenholtz and Eligehausen 2015). Other researchers have focused on anchors covering a wide range of cast-in anchor types and associated failure modes (Furche and Eligehausen 1991, Delhomme and Debicki 2010, Pallar´es and Hajjar 2010, Lee et al. 2018, Kaipei and Ožbolt 2021, Karmokar et al. 2021).

Corrosion of the steel anchors in the concrete leads to detachment of the fastened item and causes structural damage due to losses of the anchor properties. Based on accumulated experience and research that was done in order to ensure the durability of structural elements with anchors subject to corrosion, it has become more strongly recommended for the material of the insert to be resistant to corrosion (Japan Life Co., Ltd 2011). For this purpose Japan Life Co., Ltd has introduced Alumina ceramics, which is the constituent material of the Fine Ceramic Insert (FCI). It is claimed that it is a half of steel in weight, the hardest material next to diamond, and is strongly resistant to acids and alkalis. The FCI is the insert that does not corrode nor generate causes of salt damage. In addition, the FCI is already widely used for infrastructure projects in Japan, including hanging scaffoldings under the bridges, and other segmental structures. FCI is also considered for fixing the superconducting coils of Maglev. Japan Life is also consulting with JR Railway Technical Institute to do the testing of FCI for applying PC railway sleepers.

2 Scope of Work

The overall objective of this research project is to test the FCI inserts under tension and shear and compare the results to ACI318 design equations. The FCI are tested under monotonic loading conditions based on the US standard testing protocols. In the following parts, a preliminary review of the FCI anchors according to the Japan Life Co. report is presented. Design codes and guidelines for testing the anchors' performance according to the ACI code are also included. In consultation with the sponsor, the failure mode anticipated and targeted for both tension and shear tests is through concrete breakout (cone failure) though other types of failure could govern the test results as shown in **Figure 3**. As such, all specimens were designed to achieve concrete breakout failure. Furthermore, specimen had no reinforcement as directed by the sponsor. Note that specimens with thickness less than 3.0 h_{ef} (and no supplementary reinforcement), the splitting failure may occur before reaching the concrete breakout strength.The experimental program included two main steps: (1) tension tests for anchors located at the center and edge of concrete blocks, and (2) shear tests for different cases described in detail in **Section 6**. Both series of tests were performed at the UH structural laboratory based on the testing procedures in ASTM-E488. The test results should provide a good prediction behavior model of the FCI that satisfy the ACI requirements (ACI318-19) for the concrete breakout strength.

The RT who contributed to the preparation of the deliverable is composed of the Principal Investigator, Dr. Abdeldjelil Belarbi of the University of Houston, who serves as Project Manager, and Post-Doctoral Associate, Dr. Abdelmounaim Mechaala of the University of Houston.

3 Preliminary Review of FCI as reported by Japan Life Co.

According to the FCI technical report of the Japan Life Co., Ltd (2011), the FCI is very compatible with concrete and due to FCI's constituent materials, it does not corrode nor cause corrosion to occur. All of the problems inherent to date with the use of conventional metallic inserts have been resolved when using these inserts. The Japan Institute of Construction Engineering (JICE), in November 1998, awarded a Technical Evaluation Certificate to FCI for the use of FCI for hanging scaffoldings in prestressed concrete bridges. Since the beginning of its sales, FCI has been continually developed and improved to meet the changing requirements of the construction industry. All FCI products do not allow cement fluids to flow into the threaded area of inserts during concrete placement (Japan Life Co., Ltd). In 2002, the Japan Prestressed Concrete Contractors Association (JPCCA) issued the publication "Guideline for design and application of inserts for outrigger scaffoldings for wheel guards and bridge railings:" The FCI range of products that comply with the requirements of this document was updated at that time. In April 2005, JPCCA published "Guideline for Design and Application of Inserts" and the aforesaid 2002 Guideline was discontinued. Upon the occasion of the issue of this new guideline, the technical data for FCI was once again updated. In July 2005, the technical data related to the fire resistance of FCI was supplemented. In October 2008, a new integral type of FCI range was introduced: FCI was redesigned with the sleeve and body molded into one part before being fired. All of the new FCI range was tested independently by the Japan Testing Centre for Construction Materials (JTCCM). Testing of types and lengths, M12 x 60 and M16 x 65, 75, 85 were conducted. Results of the pull-out tests of the embedded inserts confirmed that the new one-piece integral FCI type had the same or equivalent strength compared to those of the previous two-part types. Also for larger sizes such as M20, M22, and M24, the integral type of FCI has been developed to meet a variety of needs. **Figure 1** shows different sizes of the one-piece integral FCI.

Figure 1. Different sizes of FCI (Japan Life Co., Ltd, 2011).

The FCI contains more than 96% of the purity of Alumina for the parts of the body. The FCI does not cause any bimetallic corrosion to steel reinforcements, and the integral wedge-shaped body secures firmly the effects of anchoring. The strength of the body at its parts having threads for the M12 and M16 (see Figure 1) are more than 11.55 kips and 21.54 kips, respectively. More details about the mounting methods and examples of uses are shown in **Figure 2**.

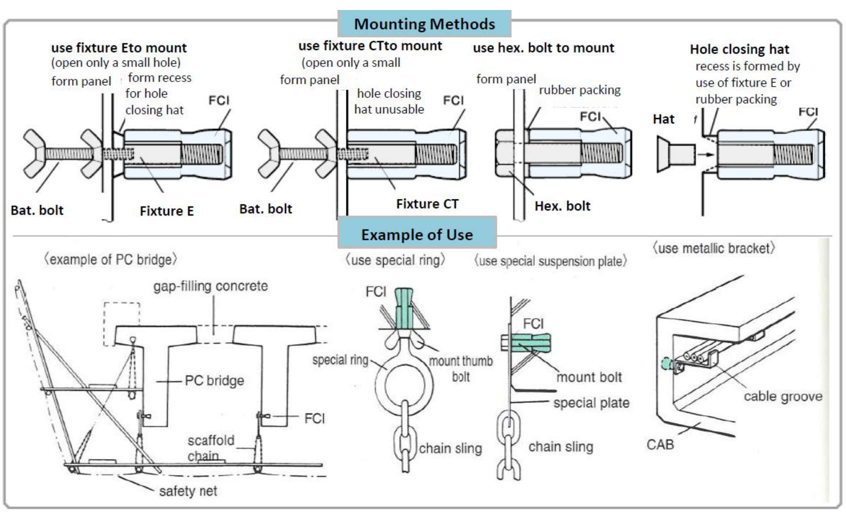

Figure 2. Mounting methods and examples of uses of FCI (Japan Life Co., Ltd, 2011).

When an external tension load is applied, the pull-out tension for FCI insert is determined by conical breaking of concrete. The design formula for various anchor bolts provided in "Indication and its exposition for designing various comprehensive structures" by Architectural Institute of Japan is given by Eq.(1):

$$Pt = \phi_1 \sqrt{\sigma_c \times 10.2} \times \pi \times L \times (L + D) \times 0.098 \tag{1}$$

Where:
Pt: Pull-out tension.
σ_c: Standard strength of concrete for design (N/mm^2).
L: Inserting depth of FCI.
D: Outer diameter of FCI (mm)
ϕ_1: Reduction coefficients (For Long term load = 0.4; For Short term load = 0.6; For JPCCA =1/3).

In the case of an externally applied shear load,the design formula is given by Eq.(2):

$$Qa = \phi \times \left(0.5 \times A_s \times \sqrt{f'_{ck} \times E_c}\right) \tag{2}$$

Where:
Qa: Shearing strength per a piece of FCI (N).
ϕ: Reduction coefficient assumed to be 0.4 and 0.6 for long/short term load respectively.
A_s: Design standard strength of concrete (N/mm).
f'_{ck}: The smaller value (mm) between the section area for the threaded parts and other parts of fixing bolt.
E_c: Young modulus for concrete.

4 Design Codes And Guidelines For Testing Anchors Performance

Different design codes cover the design of anchors embedded in concrete and provide predictions of their failure modes such as EN 1992-4 Eurocode 2 Part 4, ACI 318 Chapter 17, ACI 355, and Standards Australia committee AS 5216.

The American Concrete Institute (ACI) design code ACI 318 -19 CHAPTER 17 covers anchor design including seismic design requirements. Different types of anchors connected to concrete have been introduced by ACI in order to have good prediction models of the anchor's capacity under different load loading conditions. Typical cast-in-headed studs and headed bolts with head geometries consistent with ASME B1.1, B18.2.1, and B18.2.6 have been tested. Post-installed expansion, screw and undercut anchors pull-out strengths are established according to ACI 355.2 requirements. For adhesive anchors, the characteristic bond stress and suitability for structural applications are established by testing in accordance with ACI 355.4.

In addition, the American Society for Testing and Materials (ASTM) developed a standard and guideline for Test Methods for Strength of Anchors in Concrete and Masonry Elements ASTM E488 (2003). These test methods cover procedures for determining the static, seismic, fatigue and shock, tensile, and shear strengths of post-installed and cast-in-place anchorage systems in structural members made of concrete or structural members made of masonry. Furthermore, ASTM C900 (2020) Standard Test Method for Pullout Strength of Hardened Concrete covers the determination of the pull-out strength of hardened concrete by measuring the force required to pull an embedded metal insert and the attached concrete fragment from a concrete test specimen or structure. The insert is either cast into fresh concrete or installed in hardened concrete. This test method does not provide statistical procedures to estimate other strength properties.

4.1 DESIGN STRENGTH AND LIMITS (ACI 318-19)

4.1.1 Design Limits

4.1.1.1 Concrete

According to ACI 318-19, the compressive strength of concrete used for calculation purposes in anchor design shall not exceed 10 ksi for cast-in anchors and 8 ksi for post-installed anchors.

4.1.1.2 Anchors :

- ✓ For anchors with diameters $\boldsymbol{d_a < 4}$ in., concrete breakout strength requirements shall be considered satisfied by the design procedure.
- ✓ For adhesive anchors with embedment depth $\boldsymbol{4d_a \leq h_{ef} \leq 20d_a}$**,** the bond strength requirement shall be considered satisfied by the design procedure of bond strength of adhesive anchors in tension (ACI 318-19 (17.6.5)).
- ✓ For screw anchors with embedment depths $\boldsymbol{5d_a \leq h_{ef} \leq 10d_a}$ and $\boldsymbol{h_{ef} \geq 1.5}$***in.,*** concrete breakout strength requirement shall be considered satisfied by the design procedure of concrete breakout strength of anchors in tension and shear (ACI 318-19 (17.6.2) and (17.7.2)).

4.1.2 Design strength (ACI 318-19)

The strength of anchors shall be based on design models that satisfy ACI requirements. For each applicable factored load combination, design strength of individual anchors and anchor groups shall satisfy $\phi S_n \geq U$ where:

S_n: Nominal moment, shear, axial, torsion, or bearing strength.
ϕ: Strength reduction factor.
U: Strength of a member or cross section required to resist factored loads or related internal moments and forces in such combinations as stipulated in the ACI code. (ACI 318-19 (17.5.1)).

The Strength reduction factor ϕ for anchors in concrete shall be determinted based on the anchor strength if it is governed by steel, concrete breakout, bond, and side-face blowout, concrete pullout, or pryout strength. The strength reduction factor φ shall be in accordance with **Table 1, Table 2,** and **Table 3.**

Table 1. Anchor strength governed by steel.

Type of steel element	Strength reduction factor ϕ	
	Tension (steel)	Shear (steel)
Ductile	0.75	0.65
Brittle	0.65	0.60

Table 2. Anchor strength governed by concrete breakout, bond, and side-face blowout.

Supplementary reinforcement	Type of anchor installation	Anchor Category* From ACI 355.2 or ACI 355.4	Strength reduction factor ϕ	
			Tension (concrete breakout, bond, or side-face blowout)	Shear (concrete breakout)
Supplementary reinforcement present	Cast-in anchors	Not applicable	0.75	0.75
	Post-installed anchors	1	0.75	
		2	0.65	
		3	0.55	
Supplementary reinforcement not present	Cast-in anchors	Not applicable	0.70	0.7
	Post-installed anchors	1	0.65	
		2	0.55	
		3	0.45	

Table 3. Anchor strength governed by steel.

Type of anchor installation	Anchor Category* From ACI 355.2 or ACI 355.4	Strength reduction factor ϕ	
		Tension (concrete pullout)	Shear (concrete pullout)
Cast-in anchors	Not applicable	0.75	0.70
Post-installed anchors	1	0.65	
	2	0.55	
	3	0.45	

* Anchor Category 1 indicates low sensitivity to installation and high reliability; Anchor Category 2 indicates medium sensitivity and medium reliability; Anchor Category 3 indicates high sensitivity and lower reliability.

Different external loading can be applied to the anchor such as individual tension, individual shear, or the combination of tension and shear loading. In such cases, various types of steel and concrete failure modes for anchors presented by ACI 318-19 are shown in **Figure 3**.

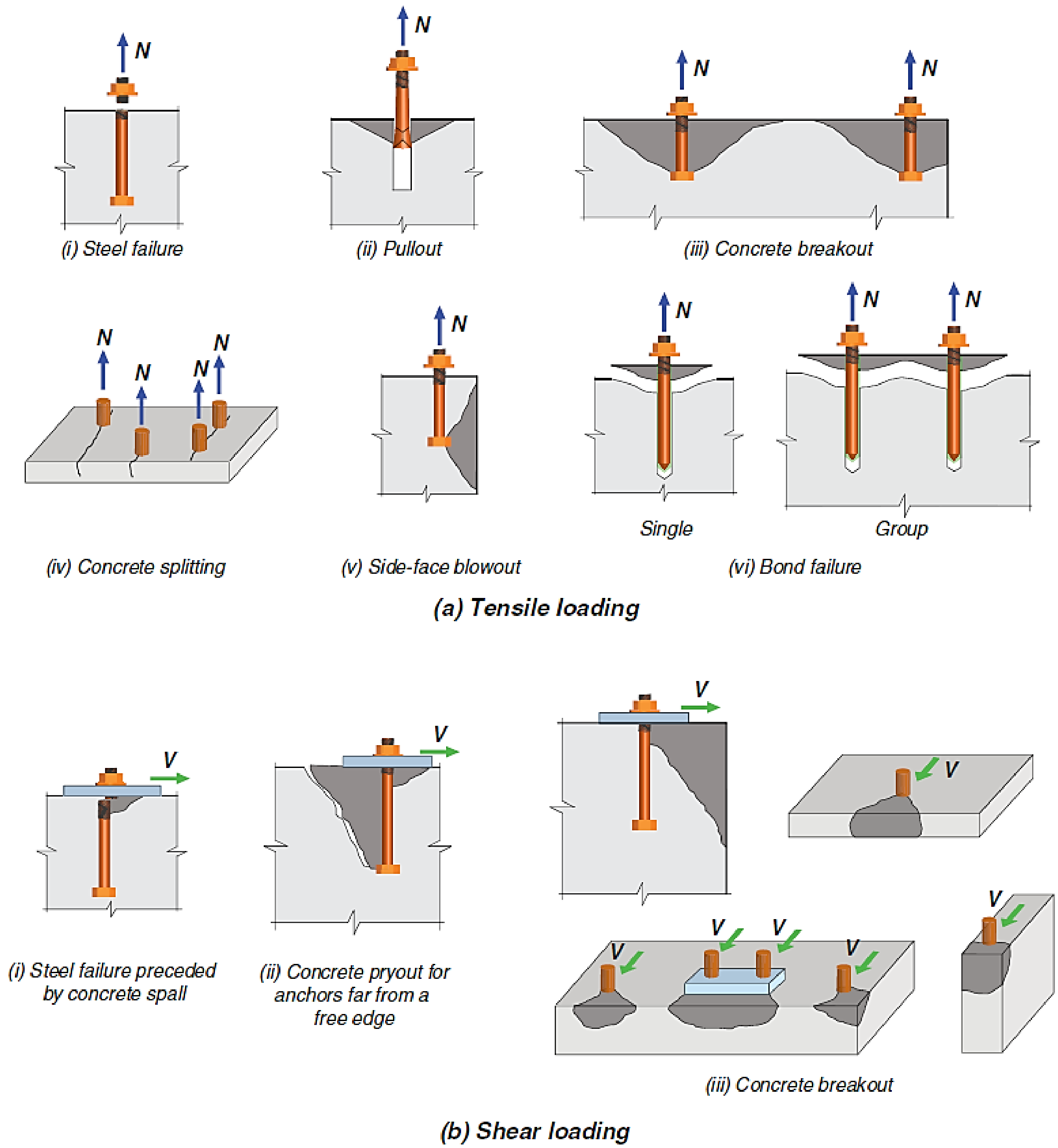

Figure 3. Failure modes for anchors (ACI 318-19).

It is therefore important to have accurate prediction models of the anchors' strength under different types of external load. The strength of anchors shall be based on design models that satisfy ACI 318-19 as presented in **Table 4**.

Table 4. Design strength requirements of anchors (ACI 318-19).

Failure mode	Single anchor	Anchor group[1]	
		Individual anchor in a group	Anchors as a group
Steel strength in tension	$\phi N_{sa} \geq N_{ua}$[2]	$\phi N_{sa} \geq N_{ua,i}$[3]	
Concrete breakout strength in tension	$\phi N_{cb} \geq N_{ua}$		$\phi N_{cbg} \geq N_{ua,g}$[4]
Pullout strength in tension	$\phi N_{pn} \geq N_{ua}$	$\phi N_{pn} \geq N_{ua,i}$	
Concrete side-face blowout strength in tension	$\phi N_{sb} \geq N_{ua}$		$\phi N_{sbg} \geq N_{ua,g}$
Bond strength of adhesive anchor in tension	$\phi N_{a} \geq N_{ua}$		$\phi N_{ag} \geq N_{ua,g}$
Steel strength in shear	$\phi V_{sa} \geq V_{ua}$	$\phi V_{sa} \geq V_{ua,i}$	
Concrete breakout strength in shear	$\phi V_{cb} \geq V_{ua}$		$\phi V_{cbg} \geq V_{ua,g}$
Concrete pryout strength in shear	$\phi V_{cp} \geq V_{ua}$		$\phi V_{cpg} \geq V_{ua,g}$

[1] Design strengths for steel and pullout failure modes shall be calculated for the most highly stressed anchor in the group.
[2] N_{ua} factored tensile force applied to anchor or individual anchor in a group of anchors, lb.
[3] $N_{ua,i}$ factored tensile force applied to most highly stressed anchor in a group of anchors, lb.
[4] $N_{ua,g}$ total factored tensile force applied to anchor group,lb.

4.1.2.1 Steel strength of anchors in tension, N_{sa} (ACI 318-19 (17.6.1))

Nominal steel strength of an anchor in tension, N_{sa}, shall be calculated by Eq.(3):

$$N_{sa} = A_{se,N} \times f_{uta} \tag{3}$$

where $A_{se,N}$ is the effective cross-sectional area of an anchor in tension, in.^{2}. For threaded rods and headed bolts, ASME B1.1 defines $A_{se,N}$ as :

$$A_{se,N} = \frac{\pi}{4}\left(d_a - \frac{0.9743}{n_t}\right)^2 \tag{4}$$

where n_t is the number of threads per inch, and d_a is the nominal diameter of bolt.

f_{uta} used for calculations shall not exceed either $1.9f_{ya}$ or 125,000 psi. The limitation of $1.9f_{ya}$ on f_{uta} is to ensure that, under service load conditions, the anchor does not exceed f_{ya} (maximum value of $f_{uta}/f_{ya}$is 1.6 for ASTM A307).

4.1.2.2 Concrete breakout strength of anchors in tension (ACI 318-19 (17.6.2)).

To compute the failure load associated with concrete cone breakout, Fuchs et al.1995 proposed the Concrete Capacity Design (CCD) method. The equation for the basic concrete breakout strength was derived assuming concrete breakout with an angle of approximately 35 degrees. The proposed method has been incorporated into ACI 318-19 as follows,
Nominal concrete breakout strength in tension, $N_{cb}$of a single anchor shall be calculated by Eq.(5)

$$N_{cb} = \frac{A_{Nc}}{A_{Nco}} \Psi_{ed,N} \Psi_{c,N} \Psi_{cp,N} N_b \tag{5}$$

Where:

A_{Nco}: is the maximum projected area for a single anchor

A_{Nc} : is the projected concrete failure area of a single anchor or of an anchor group that is approximated as the base of the rectilinear geometrical shape that results from projecting the failure surface outward $1.5h_{ef}$ ef from the centerlines of the anchor. **Figure 4** shows the calculation of A_{Nco} and A_{Nc}.

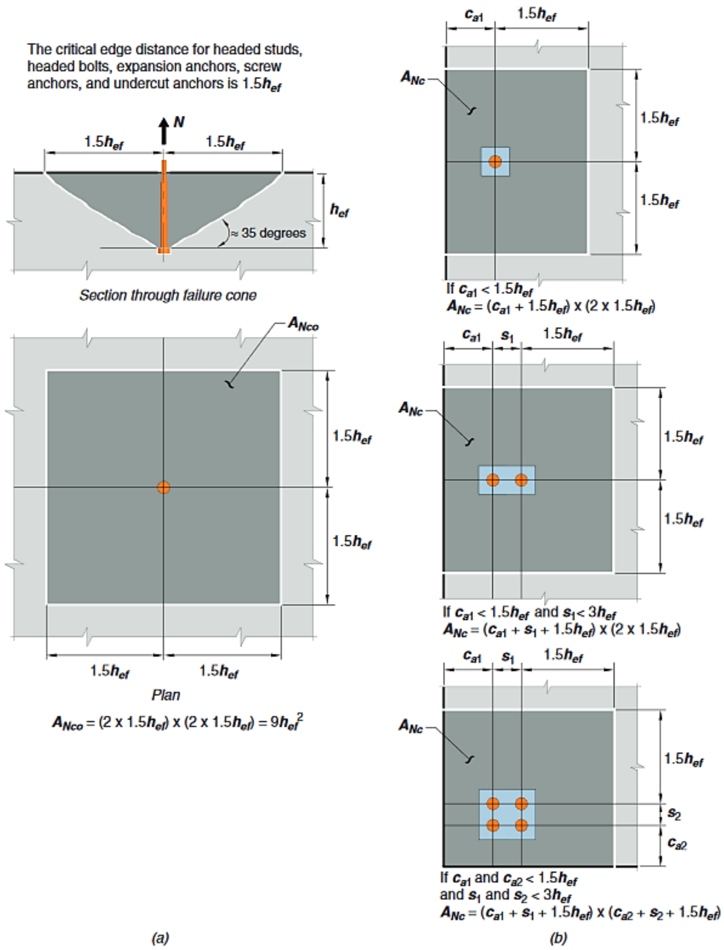

Figure 4. (a) Calculation of A_{Nco} and (b) calculation of A_{Nc} for single anchors and anchor groups (ACI 318-19).

$\Psi_{ed,N}$: Breakout edge effect factor

(a) If $c_{a,min} \geq 1.5h_{ef}$ then $\Psi_{ed,N} = 1.0$

(b) If $c_{a,min} < 1.5h_{ef}$ then $\Psi_{ed,N} = 0.7 + 0.3\frac{c_{a,min}}{1.5h_{ef}}$

$\Psi_{c,N}$:Breakout cracking factor

(a) For anchors located in a region of a concrete member where analysis indicates no cracking at service load levels:
   - $\Psi_{c,N}$= 1.25 for cast-in anchors
   - $\Psi_{c,N}$= 1.4 for post-installed anchor.

(b) For anchors located in a region of a concrete member where analysis indicates cracking at service load levels:
   - $\Psi_{c,N}$= 1.0 for both cast-in anchors and post-installed anchors.

The anchor qualification tests of ACI 355.2 or ACI 355.4 require that anchors are in cracked concrete. For these tests the anchors are considered to be in a region of cracked concrete.

$\Psi_{cp,N}$: Breakout splitting factor,.

For all other cases, including cast-in anchors, $\Psi_{cp,N}$ shall be taken as 1.0. When a tensile load is applied, the splitting failure may occur before reaching the concrete breakout strength when the member thickness is thin (Rasoul Nilforoush et al. 2017). To control the splitting failure, supplementary reinforcement might be included. For additional information Rasoul Nilforoush et al. 2017 studied the effect of member thickness and the results are shown in **Figure 5** and **Figure 6**.

(a) (b) (c)

Figure 5. Load-displacement curves of anchor bolts in NPC members of various thicknesses: (a)H $= 1.5h_{ef}$, (a)H $= 2.0h_{ef}$, (a)H $= 3.0h_{ef}$ (Rasoul Nilforoush et al. 2017).

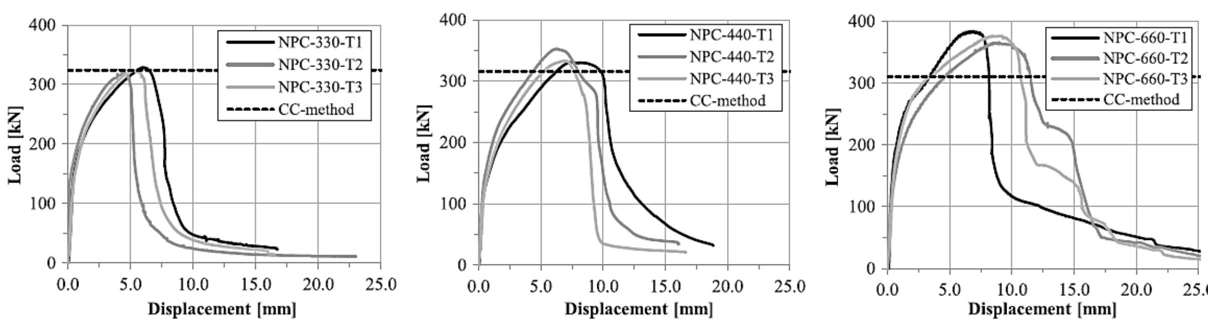

(a) (b) (c)

Figure 6. Crack pattern at failure in plain normal-strength concrete members of various thicknesses: (a)H $= 1.5h_{ef}$, (a)H $= 2.0h_{ef}$, (a)H $= 3.0h_{ef}$ (Rasoul Nilforoush et al. 2017).

N_b: Basic single anchor breakout strength,
The basic concrete breakout strength of a single anchor in tension in cracked concrete, N_b, shall be calculated by Eq.(6)

$$N_b = \mathrm{k}_c \lambda_a \sqrt{f_c'} h_{ef}^{1,5} \tag{6}$$

where k_c = 24 for cast-in anchors and 17 for post-installed anchors.

The values of k_c were determined from a large database of test results in uncracked concrete at the 5 percent fractile (Fuchs et al. 1995). The values were adjusted to corresponding kc values for cracked concrete (Elige-hausen and Balogh 1995; Goto 1971).

4.1.2.3 Pull-out strength of single cast in the anchor and single post-installed expansion, screw and undercut anchor in tension (ACI 318-19 (17.6.3)).

Nominal pullout strength of a single cast-in anchor or a single-post-installed expansion, screw, or undercut anchor in tension, N_{pn}, shall be calculated by Eq.7:

$$N_{pn} = \Psi_{c,p} N_p \tag{7}$$

Where:

$\Psi_{c,p}$: Pullout cracking factor

(a) For anchors located in a region of a concrete member where analysis indicates no cracking at service load levels :
   - $\Psi_{c,p}$= 1.4

(b) For anchors located in a region of a concrete member where analysis indicates cracking at service load levels :
   - $\Psi_{c,p}$= 1.0

N_p: Basic single anchor pullout strength
For cast-in headed studs and headed bolts, N_p shall be calculated by Eq.8:

$$N_{pn} = 8 A_{brg} f_c' \tag{8}$$

A_{brg} :is the bearing area.

4.1.2.4 Steel strength of anchor in shear (ACI 318-19 (17.7.1)).

Nominal strength of an anchor in shear, Vsa, shall not exceed (a) through (b):

a) For cast-in headed stud anchor :

$$V_{sa} = A_{se,V} f_{uta} \tag{9}$$

Where
$A_{se,V}$ is the effective cross-sectional area of an anchor in shear, in.2 (see Eq.4).

f_{uta} used for calculations shall not exceed either $1.9f_{ya}$or 125,000 psi.

b) For cast-in headed bolt and hooked bolt anchors and for post-installed anchors where sleeves do not extend through the shear plane

$$V_{sa} = 0.6A_{se,V}f_{uta} \tag{10}$$

4.1.2.5 Concrete breakout strength of anchor in shear (ACI 318-19 (17.7.2)).

Nominal concrete breakout strength in shear, V_{cb} , of a single anchor shall be calculated in accordance with (a) through (d):

$$V_{cb} = \frac{A_{vc}}{A_{vco}}\Psi_{ed,v}\Psi_{c,v}\Psi_{h,v}V_b \tag{11}$$

A_{vco} : is the maximum projected area for a single anchor that approximates the surface area of the full breakout volume for an anchor unaffected by edge distance, spacing, or depth of member.
A_{vc} :is the projected area of the failure surface on the side of the concrete member at its edge (see **Figure 7**).

$\Psi_{ed,V}$: Breakout edge effect factor

(c) If $c_{a,2} \geq 1.5c_{a1}$ then $\Psi_{ed,N} = 1.0$

(d) If $c_{a,2} < 1.5c_{a1}$ then $\Psi_{ed,N} = 0.7 + 0.3\frac{c_{a,2}}{1.5c_{a1}}$

$\Psi_{c,V}$:Breakout cracking factor

(c) For anchors located in a region of a concrete member where analysis indicates no cracking at service load levels :
   - $\Psi_{c,V}$= 1.4 for cast-in anchors

(d) For anchors located in a region of a concrete member where analysis indicates cracking at service load levels :

Table 5. Modification factor where analysis indicates cracking at service load levels

Condition	$\Psi_{c,V}$
Anchors without supplementary reinforcement or with edge reinforcement smaller than a No. 4 bar	1.0
Anchors with reinforcement of at least a No. 4 bar or greater between the anchor and the edge	1.2
Anchors with reinforcement of at least a No. 4 bar or greater between the anchor and the edge, and with the reinforcement enclosed within stirrups spaced at not more than 4 in	1.4

$\Psi_{v,N}$: Breakout thickness factor for anchors located in a concrete member where $h_a < 1.5c_{a1}$, $\Psi_{v,N}$ shall be calculated by Eq.12:

$$\Psi_{v,N} = \sqrt{\frac{1.5c_{a1}}{h_a}} \geq 1.0 \tag{12}$$

V_b: Basic single anchor breakout strength of a single anchor in shear in cracked concrete, V_b, shall not exceed the lesser of (a) and (c):

a.

$$\mathrm{V}_b = \left(7\left(\frac{l_e}{d_a}\right)^{0.2}\sqrt{d_a}\right)\lambda_a\sqrt{f_c'}(c_{a1})^{1.5} \geq 1.0 \tag{13}$$

where l_e is the load-bearing length of the anchor for shear:
$l_e = h_{ef}$ for anchors with a constant stiffness over the full length of embedded section, such as headed studs and post-installed anchors with one tubular shell over full length of the embedment depth;
$l_e = d_a$ for torque-controlled expansion anchors with a distance sleeve separated from expansion sleeve;
$l_e \leq 8d_a$ in all cases.

b.

$$\mathrm{V}_b = 9\lambda_a\sqrt{f_c'}(c_{a1})^{1.5} \geq 1.0 \tag{14}$$

c.

$$\mathrm{V}_b = \left(8\left(\frac{l_e}{d_a}\right)^{0.2}\sqrt{d_a}\right)\lambda_a\sqrt{f_c'}(c_{a1})^{1.5} \geq 1.0 \tag{15}$$

4.1.2.6 Concrete pryout strength of anchor in shear. (ACI 318-19 (17.7.3)).

Nominal pryout strength, V_{cp} of a single anchor shall not exceed Eq.16 :

$$V_{cp} = k_{cp}N_{cp} \tag{16}$$

$k_{cp} = 1.0\ for\ h_{ef} < 2.5in.$
$k_{cp} = 2.0\ for\ h_{ef} \geq 2.5in.$
For cast-in anchors and post-installed expansion, screw, and undercut anchors, N_{cp} shall be taken as N_{cb}.

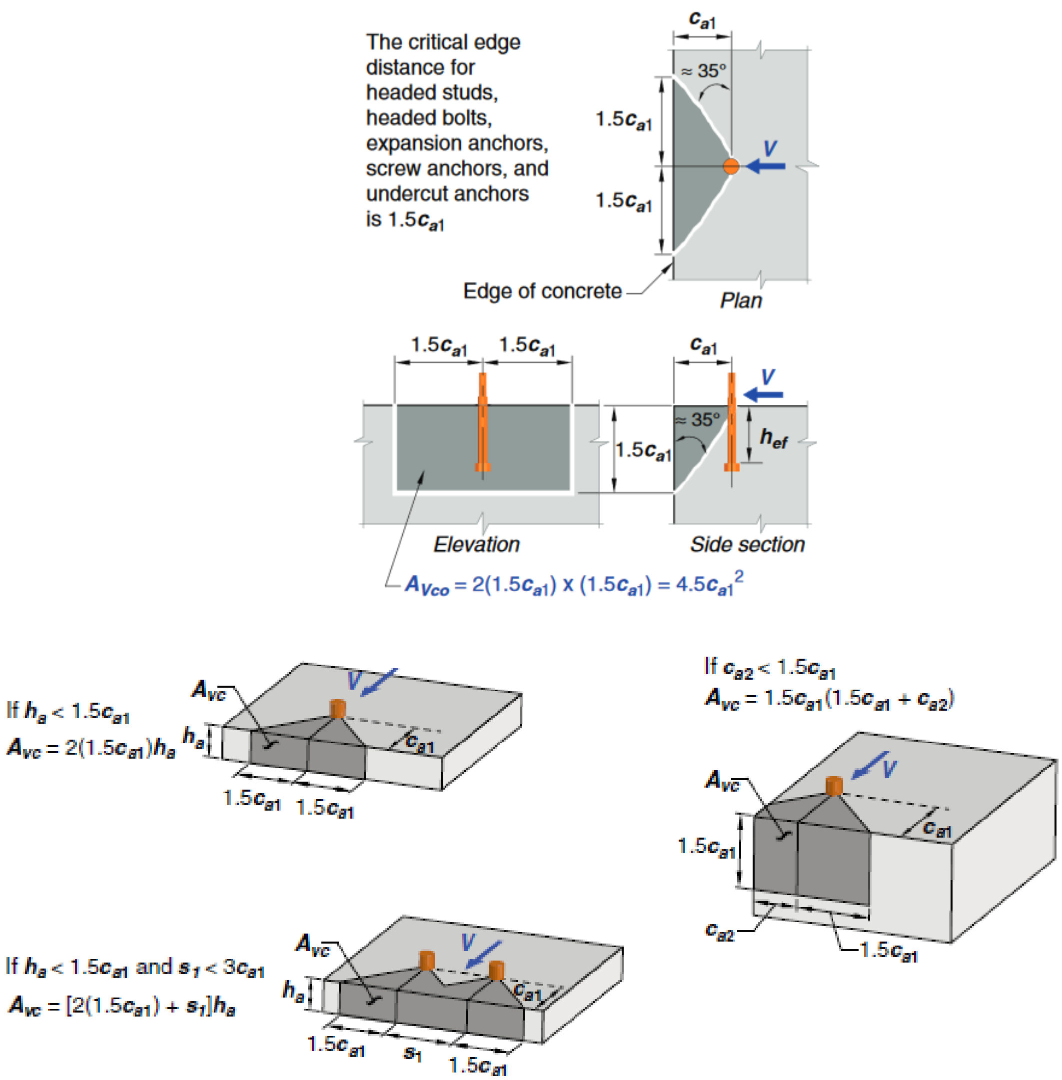

Figure 7. Calculation of A_{vco} and A_{Nc} for single anchors (ACI 318-19).

4.2 TESTING PROCEDURES (ASTM-E488-22)

ASTM E488 addresses the tensile and shear strengths of post-installed and cast-in-place anchors in test members made of cracked or uncracked concrete. These test methods provide basic testing procedures for use with product-specific evaluation and acceptance standards and are intended to be performed in a testing laboratory. Product-specific evaluation and acceptance standards may add specific details and appropriate parameters as needed to accomplish the testing. Only those tests required by the specifying authority need to be performed. These test methods are intended for use with the FCI insert.

4.2.1 Tension Test Equipment(ASTM-E488-22)

The support for the tension test equipment shall be of sufficient size to prevent failure of the surrounding test member. The displacement measuring device(s) shall be positioned to measure the movement of the anchors with respect to points on the test member so that the device is not influenced during the test by deflection or failure of the anchor or test member. According to ASTM-E488-22, the minimum required clear distance from the test support to the anchor for loading is presented in **Table 6**. **Figure 8** presents an example of a typical test setup for tension test.

Table 6. Minimum Clearance Requirements for Test Equipment Supports (Tension Loads)

All Anchors		
Tension Loads	Spacing Between Test Supports	Distance from Anchor to Edge of Test Support
	4.0 h_{ef}	2.0 h_{ef}

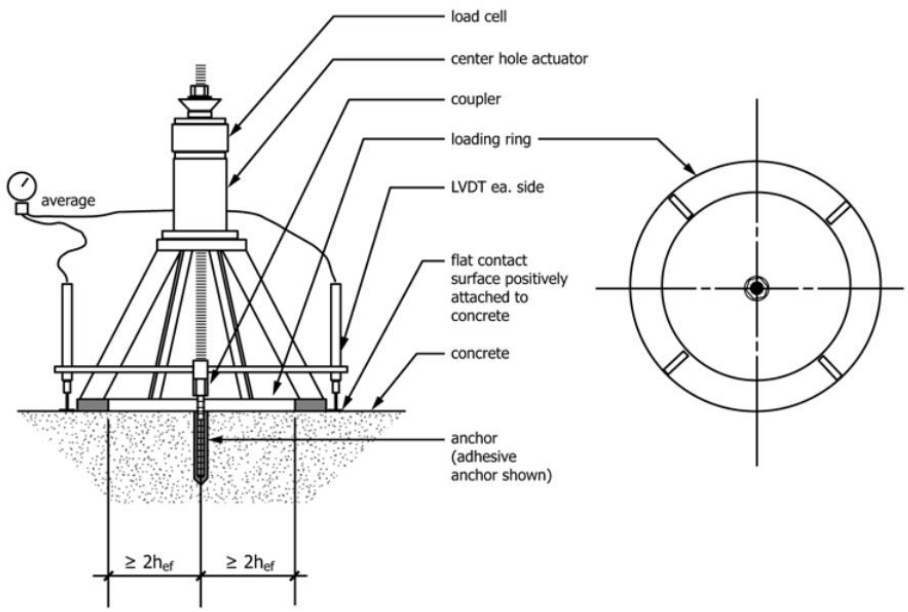

Figure 8. Example of Unconfined Tension Test Setup – Displacement Measurement with Dual LVDTs (ASTM E488, 2003).

4.2.2 Shear Test Equipment (ASTM-E488-22)

ASTM-E488 requires that the displacement measuring device(s) should be positioned to measure displacement in the direction of the applied load only. The device should be placed on the test member so that the sensing element bears perpendicularly on the anchor or on a contact plate located on the loading plate, or using another method that restricts deflections other than those in the direction of the applied load. According to ASTM-E488-22, the minimum required clear distance from the test support to the anchor shear loading toward a free edge is presented in **Table 7**. **Figure 9** presents and example of a typical test setup for shear tests.

Table 7. Minimum Clearance Requirements for Test Equipment Supports (Shear Loads)

All Anchors		
Tension Loads	Spacing Between Test Supports	Distance from Anchor to Edge of Test Support
	4.0 c_a	2.0 c_c

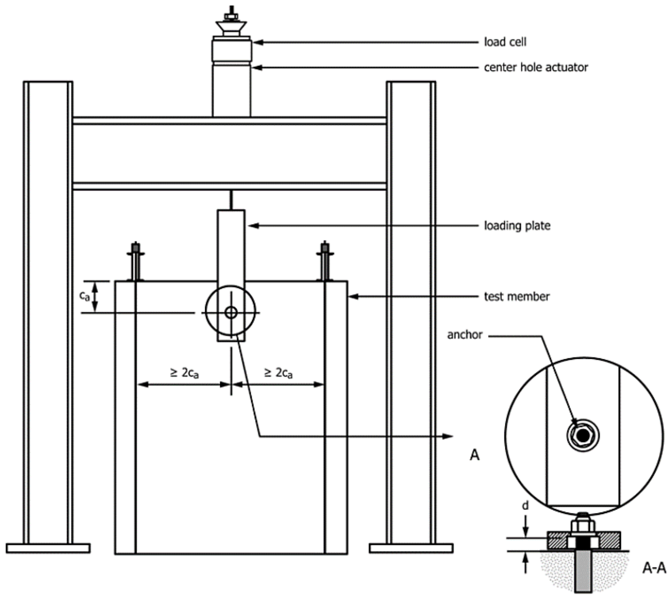

Figure 9. Example of a Shear Test Setup (ASTM E488, 2003).

For tension and shear loading, the plate thickness, t_{fix} , of the test anchor shall be equal to or greater than the nominal anchor diameter to be tested.

4.2.3 Testing Specimens and loading protocol

The minimum number of replicate anchor test specimens shall be specified as part of the testing program. For tension and shear tests, three repetitions for each insert type will be used.

Two different *loading rates* were selected according to ASTM-E488

- Initial Load: apply an initial load up to 5 % of the estimated maximum load capacity of the anchorage system to be tested, in order to bring all members into full bearing.
- Rate of Loading: two loading rates are given.The first method requires a continuous increase in load up to failure or up to a maximum specified load or displacement (a minimum 1-min total test time and a maximum 3-min). The second is a step-loading method in 15 % increments of the expected ultimate load. For tests that require precise anchor load-displacement data for calculating stiffness or assessing proper functioning, the continuous load application method is required.

5 Analytical analysis for FCI according to ACI 318-19

5.1 Expected Failure modes for FCI

In this investigation, revised provisions will be proposed for the use of FCI insert according to the ACI Design Code. The main expected failure mode is concrete breakout (cone failure) for both tensile and shear tests. The steel anchor failure is not applicable for FCI tests since the purpose of this research is to study the effectiveness of the FCI insert independent of the anchor strength. For this reason, high-strength threaded rods were used. Furthermore, the members with thickness less than 3.0 h_{ef} (and no supplementary reinforcement), the splitting failure may occur before reaching the concrete breakout strength. **Table 8** shows the expected and the improbable mode of failure for the FCI tests.

Table 8. The expected and improbable mode of failure for the FCI Test.

Expected Failure Modes for FCI	Improbable Failure Modes for FCI
➢ Concrete Breakout (center) ➢ Side-Face Blowout (edge) ➢ Concrete Splitting (when the thickness less then 3.0 h_{ef})	➢ Steel Failure (center/edge): High- Strength threaded rods will be used. ➢ Bond Failure (center/edge): Evaluation of bond strength applies only to adhesive anchors. ➢ Pullout Failure (center/edge): requires higher loading.

5.2 THE SHAPE AND SPECIMEN SIZE

The specimens' sizes followed the procedures indicated in ASTM-E488 (Standard Test Methods for Strength of Anchors in Concrete Elements) and the minimum requirements of ACI 318-19. Three FCI inserts were used for this study (FCI 1/2 in.- FCI 5/8 in.- FCI 1 in.). More details about the chosen FCI and their standard dimensions are shown in **Figure 10**. The dimensions of the specimens for the tension and shear tests are presented in **Table 9** and **Table 10**.

■FCI

Dimensional drawing

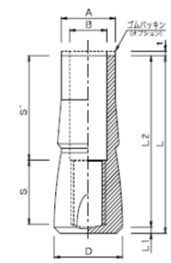

■Standard Dimensions

in mm

Product's Code (FCI-)	Screw	FCI (Main body)								Packing/Option		Remarks
		L	L1	L2	D	A	B	S	S'	t		
M10N x 43	M10	43	2	41	22	17	11	18.5	23.5	1		
M12N x 60	M12	59.5	2	57.5	24	19	13	21.5	35	1.5	5	
M12N x C4	M12	79	2	77	24	19	13	21.5	54.5	1.5	5	For JPCCA
M16N x 65	M16	65.5	2	63.5	33	25	17	24	38.5	2	5	
M16 x 75	M16	75.5	2	73.5	33	25	17	24	48.5	2	5	
M16N x 85	M16	85.5	2	83.5	33	25	17	24	58.5	2	5	
M16N x C111	M16	106	2	104	33	25	17	24	79	2	5	For JPCCA
M20N x 100	M20	100	3	97	42	28	21	33	63	2		
M22N x 110	M22	110	4	106	45	31	23	37	69	2		
M24N x 120	M24	120	4	116	50	33	25	40	75	2		

(a): Standard dimensions

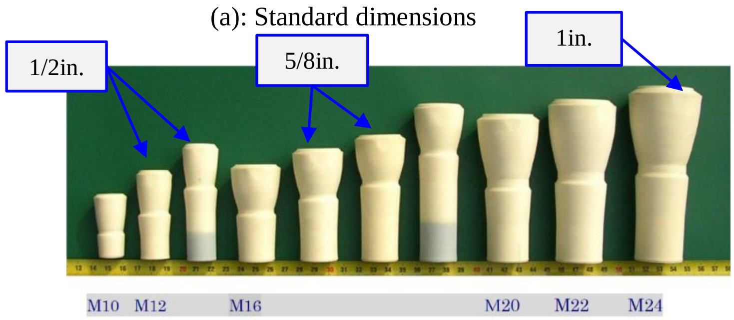

(b) : FCI inserts chosen

Figure 10. Standard dimensions of the FCI (Japan Life Co., Ltd, 2011).

Table 9. The shape and size of the specimens for the tension tests.

Specimen Shape and Size Tension Test (Center)	**Specimen Shape and Size Tension Test (Edge)**
Insert Type : **FCI** 1/2in.**- FCI** 5/8in.**- FCI** 1in.	*Insert Type :* **FCI** 1/2in.**- FCI** 5/8in.**- FCI** 1in.
Total number of specimens: **18**	Total number of specimens: **18**
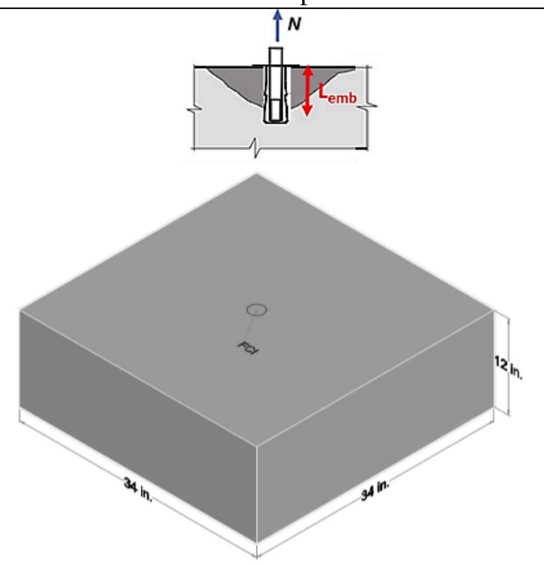	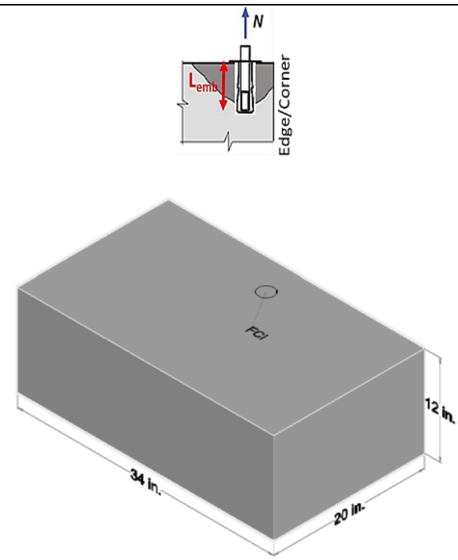

Table 10. The shape and size of the specimens for the shear tests.

Specimen Shape and Size Shear Test ($h_a < 1.5C_{a1}$)	**Specimen Shape and Size Shear Test ($h_a > 1.5C_{a1}$)**
Insert Type : **FCI** 1/2in.**- FCI** 5/8in.	*Insert Type :* **FCI** 1/2in.**- FCI** 5/8in.
Total number of specimens: ***12***	*Total number of specimens:* ***12***
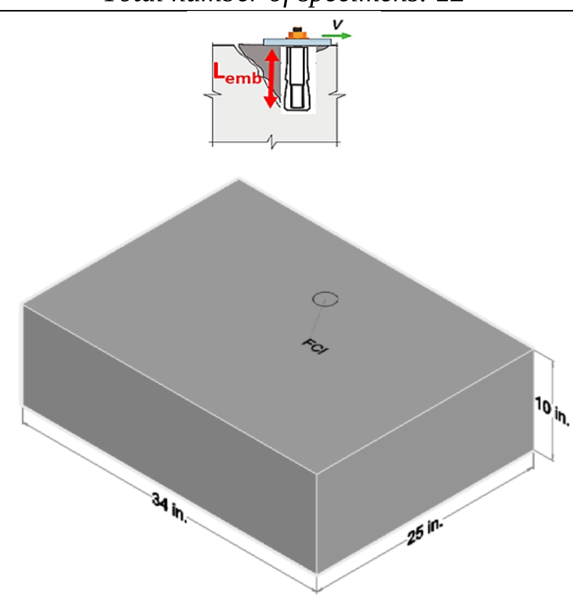	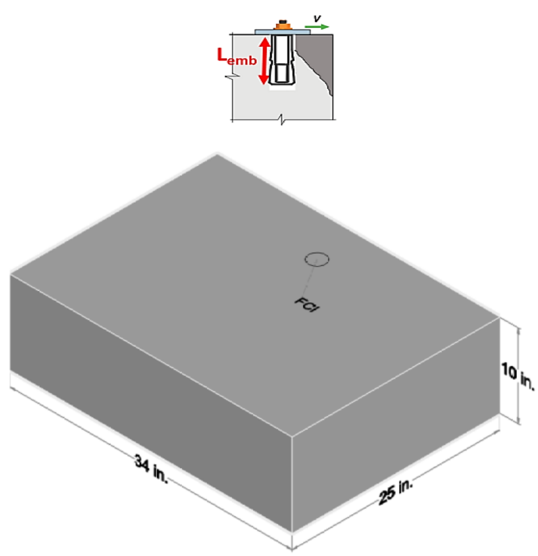

Insert Type : **FCI** 1in.	*Insert Type :* **FCI** 1in.
Total number of specimens: ***06***	*Total number of specimens:* ***06***
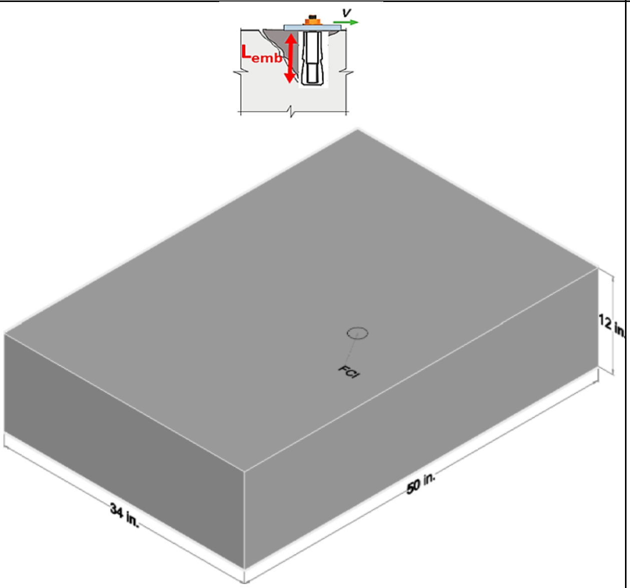	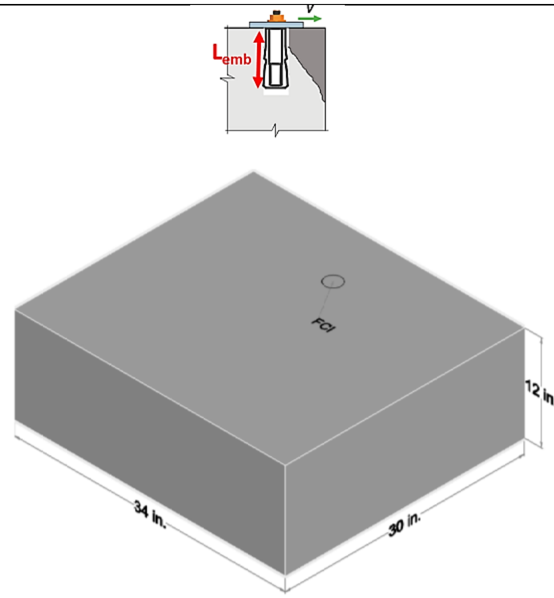

5.3 ACI 318-19 PREDICTION

The ACI prediction of the concrete breakout strength of FCI inserts in tension and shear are summarized in **Table 11** and **Table 12**, respectively. The details regarding the experimental data of the concrete strength is used in this section to validate the prediction equation. Eq.5 and Eq.11 described above will be used to calculate the nominal concrete breakout strength in tension, N_{cb} and in shear V_{cb}.

Table 11. The ACI prediction of the concrete breakout strength of FCI insert in tension.

Test	FCI Type	h_{ef}	Location	f'_c (ksi)	A_{Nco} (in^2)	A_{Nc} (in^2)	$\Psi_{ed,N}$	$\Psi_{c,N}$	$\Psi_{cp,N}$	N_b (kips)	N_{cb} (kips)
Tension	FCI1/2in.	$2^{3/8''}$	Center	3.8	49.28	49.28	1.0	1.0	1.0	5.30	**5.30**
			Edge	4.0	49.28	41.07	0.9	1.0	1.0	5.43	**4.07**
		$3^{1/8''}$	Center	3.8	87.05	87.05	1.0	1.0	1.0	8.11	**8.11**
			Edge	4.0	87.05	72.54	0.9	1.0	1.0	8.32	**6.24**
	FCI5/8in.	$3''$	Center	4.5	79.39	79.39	1.0	1.0	1.0	8.24	**8.24**
			Edge	3.8	79.39	66.16	0.9	1.0	1.0	7.57	**5.68**
		$3^{3/8''}$	Center	4.5	102.21	102.21	1.0	1.0	1.0	9.96	**9.96**
			Edge	3.8	102.21	85.18	0.9	1.0	1.0	9.15	**6.86**
	FCI1in.	$4^{3/4''}$	Center	4.5	200.51	200.51	1.0	1.0	1.0	15.37	**15.73**
			Edge	4.0	200.51	167.09	0.9	1.0	1.0	15.57	**11.67**
		$5^{1/2''}$	Center	4.5	273.24	273.24	1.0	1.0	1.0	20.82	**20.82**
			Edge	4.0	273.24	227.70	0.9	1.0	1.0	19.63	**14.72**

Table 12. The ACI prediction of the concrete breakout strength of FCI insert in shear.

Test	FCI Type	h_{ef}	Location	f'_c (ksi)	A_{Nco} (in^2)	A_{Nc} (in^2)	$\Psi_{ed,v}$	$\Psi_{c,v}$	$\Psi_{h,v}$	V_b (kips)			V_{cb} (kips)
										Eq.13	Eq.14	Eq.15	
Shear	FCI 1/2in.	$2^{3/8''}$	$h_a < 1.5C_{a1}$	3.9	220.5	210	1.0	1.0	1.02	8.68	10.41	9.92	**9.07**
			$h_a > 1.5C_{a1}$	4.6	112.5	112.5	1.0	1.0	1.0	5.69	6.82	6.6.50	**5.69**
		$3^{1/8''}$	$h_a < 1.5C_{a1}$	3.9	220.5	210	1.0	1.0	1.02	8.68	10.41	9.92	**9.07**
			$h_a > 1.5C_{a1}$	4.6	112.5	112.5	1.0	1.0	1.0	5.69	6.82	6.6.50	**5.69**
	FCI 5/8in.	$3''$	$h_a < 1.5C_{a1}$	3.9	220.5	210	1.0	1.0	1.02	9.70	10.41	11.09	**10.14**
			$h_a > 1.5C_{a1}$	4.6	112.5	112.5	1.0	1.0	1.0	6.36	6.82	7.27	**6.36**
		$3^{3/8''}$	$h_a < 1.5C_{a1}$	3.9	220.5	210	1.0	1.0	1.02	9.70	10.41	11.09	**10.14**
			$h_a > 1.5C_{a1}$	4.6	112.5	112.5	1.0	1.0	1.0	6.36	6.82	7.27	**6.36**
	FCI 1in.	$4^{3/4''}$	$h_a < 1.5C_{a1}$	4.9	364.5	324	1.0	1.0	1.06	20.05	17.01	22.92	**16.04**
			$h_a > 1.5C_{a1}$	4.0	220.5	220.5	1.0	1.0	1.0	12.43	10.54	14.20	**10.54**
		$5^{1/2''}$	$h_a < 1.5C_{a1}$	4.9	364.5	324	1.0	1.0	1.06	20.05	17.01	22.92	**16.04**
			$h_a > 1.5C_{a1}$	4.0	220.5	220.5	1.0	1.0	1.0	12.34	10.54	14.20	**10.54**

The concrete breakout strengths in tension using the design formula (given in Eq.1) for various anchor bolts provided in "Indication and its exposition for designing various comprehensive structures" by Architectural Institute of Japan are presented in **Table 13**.

Table 13. The pull-out tension for FCI prediction based on JPCCA in tension.

Test	FCI Type	h_{ef}	Location	N_{cb} (kips)
Tension	FCI1/2in.	$2^{3/8''}$	Center	**5.29**
		$3^{1/8''}$	Center	**8.79**
	FCI5/8in.	$3''$	Center	**9.63**
		$3^{3/8''}$	Center	**11.97**
	FCI1in.	$4^{3/4''}$	Center	**23.68**
		$5^{1/2''}$	Center	**31.11**

6 Experimental program

To evaluate the performance and the design of FCI in the USA, a comprehensive research program involving different monotonic loading tests (tension and shear) were performed based on the American Society for Testing and Materials for Anchors (ASTM E488). The test results should provide an accurate prediction behavior model of the FCI that satisfy the ACI requirements (ACI318-19). The influence of the mounting position and the insert depth on the failure mode and the capacity of the insert is discussed in this section.

6.1 TEST MATRIX AND FABRICATION OF TEST SPECIMENS

A total of 77 specimens were cast at Legacy Precast LLC located in Brookshire, TX. The form used to cast the specimens consisted of a steel casting bed with two steel plates welded on each side and positioned based on the required dimensions of the FCI specimens. Wooden bulkheads were used as separation between each specimen (see **Figure 11(a)**). The objective of using the steel angle as shown in **Figure 11** is to position the FCI insert in the chosen location within the concrete block. For each specimen, careful effort was made to ensure the position of the insert. The bottom and sides of the casting bed were then cleaned and sprayed with lubricant (see **Figure 11(b)**). To cast the specimens, ready-mix concrete utilizing an in-house 4.3 ksi self-consolidating concrete mix was provided by Legacy Precast LLC. Concrete was poured from the ready-mix truck into the specimens from one end of the casting bed to the other (see **Figure 11(c)**). Finally, two lift inserts were positioned around each specimen for removal, handling, and transportation of the specimens (see **Figure 11(d)**).

Figure 11. a) Adjustment of the specimen forms and position of the insert; **b)** casting bed cleaned and sprayed with lubricant; **c)** concrete being poured into the forms; **d)** position of the lift inserts.

Pull-out tension tests of the FCI were performed for two different anchor locations (center and edge) using three FCI insert sizes. Three test repetitions were done for each FCI type, which meet the minimum requirement to calculate a coefficient of variation (**see Table 14**). Similarly, for the shear tests, three FCI inserts were used (**FCI** 1/2in.- **FCI** 5/8in.- **FCI** 1in.) for two different cases ($h_a < 1.5C_{a1}$ and $h_a > 1.5C_{a1}$) as outlined in **Table 15**. More details about the standard dimensions and the chosen FCI are shown in **Figure 10.** Standard dimensions of the FCI (Japan Life Co., Ltd, 2011)..

Table 14. Details for specimens with FCI inserts subject to tension loads.

	Embedment depth of anchor		Specimens Dimensions						Specimens Dimensions			
Insert Type	L_{emb} (h_{ef}) (in.)	L_{emb} (h_{ef}) (mm)		a(in.)	b(in.)	h (in.)	Clear Distance between Supports	ASTM Check ($4{*}h_{ef}$)		a(in.)	b(in.)	h (in.)
FCI 1/2"	2.34	59.5	Tension (Center)	34	34	12	24	9.36	Tension (Edge)	20	34	12
	3.11	79		34	34	12	24	12.44		20	34	12
FCI 5/8"	2.97	75.5		34	34	12	24	11.88		20	34	12
	3.37	85.5		34	34	12	24	13.48		20	34	12
FCI 1"	4.72	120		34	34	12	24	18.88		20	34	12
	5.51	140		34	34	12	24	22.04		20	34	12

Table 15. Details for specimens with FCI inserts subject to shear loads.

	Embedment depth of anchor		Specimens Dimensions									
Insert Type	L_{emb} (h_{ef}) (in.)	L_{emb} (h_{ef}) (mm)		a(in.)	b(in.)	h (in.)	C_{a1}(in.)		a(in.)	b(in.)	h (in.)	C_{a1}(in.)
FCI 1/2"	2.34	59.5	**Shear (h_a<*1.5*C_{a1})**	25	34	10	7	**Shear (h_a>*1.5*C_{a1})**	25	34	10	5
	3.11	79		25	34	10	7		25	34	10	5
FCI 5/8"	2.97	75.5		25	34	10	7		25	34	10	5
	3.37	85.5		25	34	10	7		25	34	10	5
FCI 1"	4.72	120		34	50	12	9		30	34	12	7
	5.51	140		34	50	12	9		30	34	12	7

The specimens outlined in **Table 14** corresponding to the FCI 1" with an anchor depth of 5.51 in. have a thickness less than 3 h_{ef}. For such cases, splitting failure is expected before reaching the concrete breakout strength (Rasoul Nilforoush et al. 2017). To avoid the splitting failure, additional specimens with adjusted dimensions were cast. Furthermore, two additional specimens for FCI 4.72 in. where cast to replace the main specimens which were damaged during transportation from the precast plant to the laboratory. **Table 16** summarizes the additional specimens.

Table 16. Summary of the additional specimens for FCI 1" tension test

<table>
<tr><td rowspan="3">Insert Type</td><td colspan="2">Embedment depth of anchor</td><td colspan="5">Specimens Dimensions</td></tr>
<tr><td colspan="2">L_{emb} (h_{ef})</td><td rowspan="4">Tension (Center)</td><td rowspan="2">a(in.)</td><td rowspan="2">b(in.)</td><td rowspan="2">h (in.)</td><td rowspan="2">Number of Specimens</td></tr>
<tr><td>(in.)</td><td>(mm)</td></tr>
<tr><td rowspan="2">FCI 1"</td><td>4.72</td><td>120</td><td>34</td><td>34</td><td>12</td><td>2</td></tr>
<tr><td>5.51</td><td>140</td><td>34</td><td>34</td><td>18</td><td>3</td></tr>
</table>

As shown in **Table 14** and **Table 15**, the concrete block dimensions depend on the FCI depth and all the tests were performed on single anchors.

6.2 MATERIAL AND MECHANICAL PROPERTIES

6.2.1 FCI

As mentioned in the preliminary review, the FCI contains more than 96% of the purity of Alumina, for the parts of the body. The FCI does not cause any bimetallic corrosion to steel reinforcements, and the integral wedge-shaped body secures firmly the effects of anchoring. The strength of the body at the parts that have threads for the FCI 1/2" and FCI 1" are more than 11.55 kips and 21.54 kips respectively. **Table 17** presents the mechanical properties of the Alumina sintered body.

Table 17. Mechanical properties of Alumina sintered body (Japan Life Co., Ltd).

Item	Unit	Value
Hardness	kN	12.7
Flexural Strength	N/mm^2	398
Compressive Strength	N/mm^2	2160
Young Modulus	N/mm^2	3.17×10^7
Poisson Ratio	-	0.227
Unit Weight/Volume	g/cm^3	3.8

6.2.2 Concrete and Steel anchors

For each concrete batch used for casting the specimens, 4" x 8" cylinder samples were prepared for compression strength tests. First, the samples were demolded and then both surfaces were grinded prior to testing. All measurements were performed using a compressive strength machine (see **Figure 12**) using a controlled loading rate of 400 ± 20 Lb/s, according to ASTM C39/39M. The 77 specimens were cast in six batches. The summarized results of the maximum applied compressive force (F_c) and compressive strength (fc) are presented in **Table 19** (fc is presented separately for each casting period as well as the mean values and corresponding standard deviations for all investigated batches). In most cases, diagonal fracture with cracking through one end or columnar vertical cracking occurred at failure.

Figure 12. Setup of the compressive strength tests.

Table 18. Results of maximum load (F_c) and compressive strength (f_c) for each sample as well as the mean values ($f_{c,av}$) and corresponding standard deviations ($f_{c,st.dev}$) for both investigated concrete batches.

	Casting	Testing	Curing time (days)	Sample	D_1 [in]	D_2 [in]	D_3 [in]	D_4 [in]	D_{av} [in]	H_1 [in]	H_2 [in]	H_{av} [in]	F_c [Lb]	f_c [psi]	$f_{c,av}$ [psi]	$f_{c,st.dev}$ [psi]
FCI 1	2/20/2023	3/20/2023	**28**	**#01**	4.04	4.04	4.00	4.00	**4.02**	7.80	7.80	**7.80**	59030	4654	**4499**	**123**
				#02	4.00	4.01	4.01	4.00	**4.01**	7.80	7.80	**7.80**	54850	4353		
				#03	4.00	4.01	4.00	3.99	**4.00**	7.80	7.80	**7.80**	56405	4490		
FCI 2	2/23/2023	3/23/2023	**28**	**#01**	4.02	4.00	4.00	3.99	**4.00**	7.80	7.80	**7.80**	48355	3851	**3828**	**19**
				#02	4.00	4.00	4.00	4.01	**4.00**	7.90	7.90	**7.90**	47895	3806		
				#03	4.01	3.99	4.00	4.00	**4.00**	7.80	7.80	**7.80**	48050	3828		
FCI 3	2/28/2023	3/20/2023	**20**	**#01**	4.04	4.04	4.00	4.00	**4.02**	7.80	7.80	**7.80**	49395	3895	**4013**	**84**
				#02	4.00	4.01	4.01	4.00	**4.01**	7.80	7.80	**7.80**	51460	4084		
				#03	4.00	4.01	4.00	3.99	**4.00**	7.80	7.80	**7.80**	51010	4061		
FCI 4	2/28/2023	3/28/2023	**28**	**#01**	4.02	4.00	3.98	3.98	**4.00**	7.87	7.87	**7.87**	61495	4906	**4947**	**192**
				#02	3.98	3.99	4.06	4.00	**4.01**	7.87	7.94	**7.91**	59735	4736		
				#03	3.96	3.99	4.03	4.01	**4.00**	7.87	7.87	**7.87**	65270	5248		
FCI 5	3/29/2023	4/26/2023	**28**	**#01**	3.98	4.02	3.99	3.98	**3.99**	7.75	7.75	**7.75**	50260	3980	**3952**	**47**
				#02	4.03	4.02	3.97	3.99	**4.00**	7.69	7.69	**7.69**	48645	3886		
				#03	4.02	4.05	3.97	3.97	**4.00**	7.63	7.63	**7.63**	50195	3989		
FCI 6	3/30/2023	4/27/2023	**28**	**#01**	4.03	4.01	3.99	4.00	**4.01**	7.75	7.81	**7.78**	55825	4426	**4574**	**118**
				#02	3.99	4.03	3.99	3.99	**4.00**	7.94	7.94	**7.94**	59240	4714		
				#03	4.02	3.97	3.99	4.00	**4.00**	7.94	7.94	**7.94**	57420	4581		

High-strength bolts (Grade BD) were used for testing with the FCI 1/2in. and FCI 5/8in. while high-strength threaded rods (Grade F1554 GR 105) were used with the FCI 1in.. **Table 19** presents the mechanical properties for the threaded rod and bolts used. The ACI prediction of the steel strength of anchors in tension and shear based on Eq.3 and Eq.9-10, respectively, are summarized in **Table 20**. For FCI 1/2in., the steel strength is close to the concrete breakout strength of the FCI insert in shear. Thus, the steel failure may occur before reaching the concrete breakout strength for the case of *ha <1.5Cal*.

Table 19. Specified Mechanical Properties for the used threaded rod and bolts.

Location	Grade/ Specification	Nominal size (in.)	Tensile Strength Min (psi)	Yield Strength Min (psi)
	ASTM A354 Grade BD	1/4″ - 2-1/2″	150,000	130,000
		> 2-1/2″ - 4″	140,000	120,000
	ASTM F1554 Grade 105	All size	125,000 - 150,000	105,000

Table 20. The ACI prediction of the steel strength of anchor in tension and shear.

FCI Type	Test	Steel strength of anchor (kips)		
		Eq.3	Eq.9	Eq.10
FCI1/2in.	Tension	17.74		
	Shear		14.74	**10.64**
FCI5/8in.	Tension	28.25		
	Shear		28.25	**16.95**
FCI1in.	Tension	75.72		
	Shear		75.72	**45.43**

6.3 EXPERIMENTAL SETUP AND TESTING PROTOCOL

The experimental procedure was performed using a hydraulic jack fixed on the top of a steel frame which was anchored to the strong-floor of the Univeristy of Houston structural laboratory. Load measurements were recorded using OMEGA load cells. String potentiometers and linear variable displacement transducers (LVDTs) were used to measure the displacement of the insert. All sensors were connected to a VISHAY System 7000 Data Acquisition System which recorded continuous measurements from each sensor throughout the duration of the test.

6.3.1 Tension Test

In the tension tests, a hydraulic jack with a 100-kip load capacity was used to load the specimens in tension. The load cell was attached to the top of the hydraulic jack to measure the applied force. The load was increased in accordance with ASTM. E488M – 22 until the failure of the specimen.

The experimental setup for evaluating FCI capacity in tension is shown in **Figure 13** and **Figure 15**.

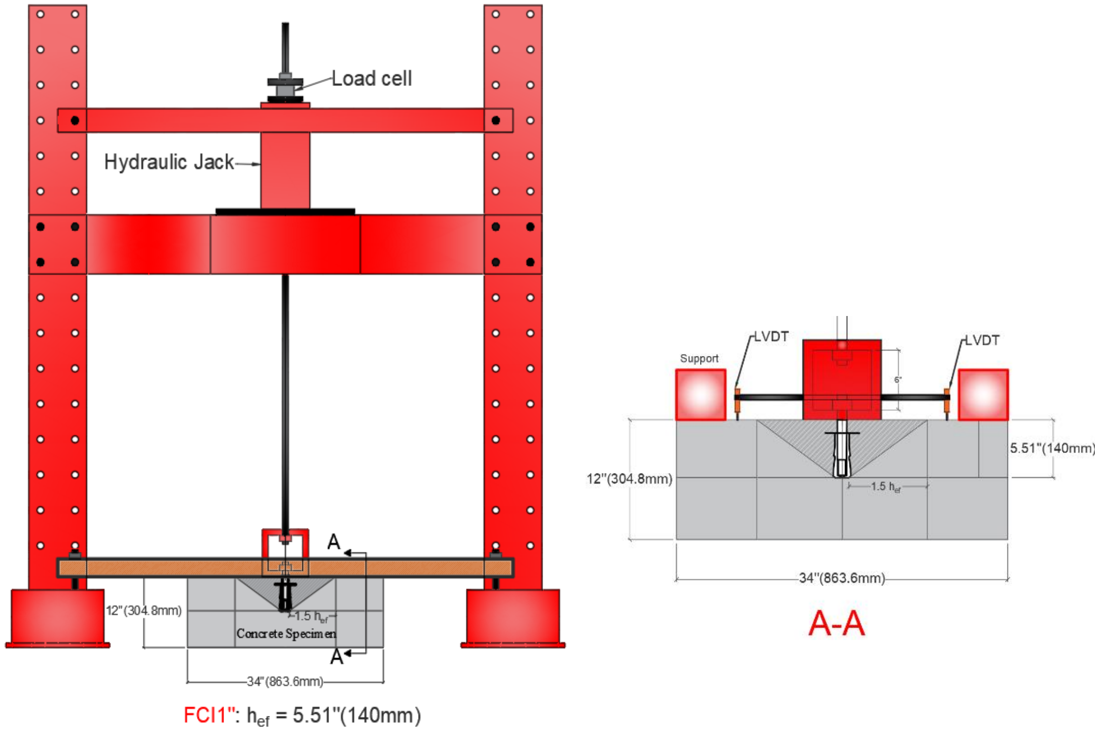

Figure 13. Planned experimental setup for tension tests (including boundary conditions, sensor positions, and specimen position).

To prepare the specimens for testing, the first step was to position the specimen below the hydraulic jack and on its supports (**Figure 14(a)**). Centerlines were marked at the proper locations on the floor of the lab using lasers and chalk-lines. Lead pads were used at the points of load application to obtain a smooth interface between the surface of the specimens and the supporting elements (HSS members were used as support elements as shown in **Figure 14(b)**). In addition, LVDTs were mounted at the level of the coupler as shown in **Figure 14**(**c**). The final experimental setup is shown in **Figure 15**. **Figure 16** shows a schematic view of the pullout tension test for the two different anchor locations (center and edge).

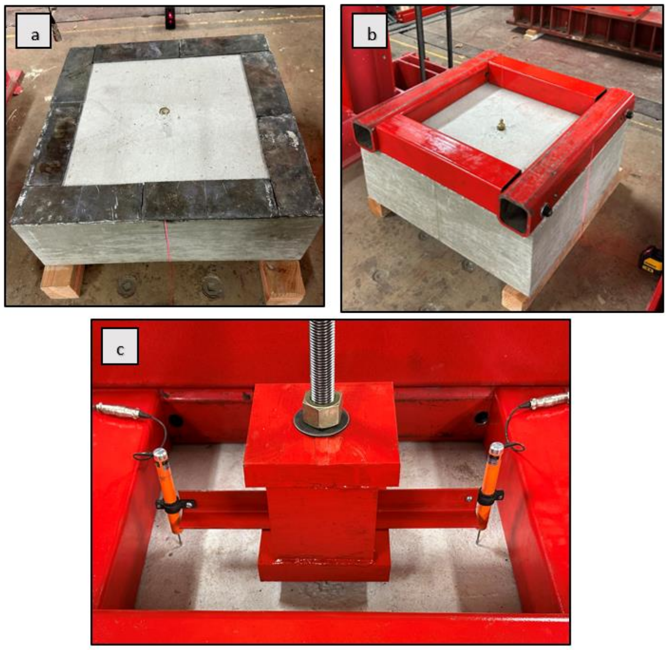

Figure 14. a) Positioning of the specimen; **b)** Positioning of the supports; **c)** LVDT mounting at the level of the coupler.

Figure 15. Experimental setup for the tension test.

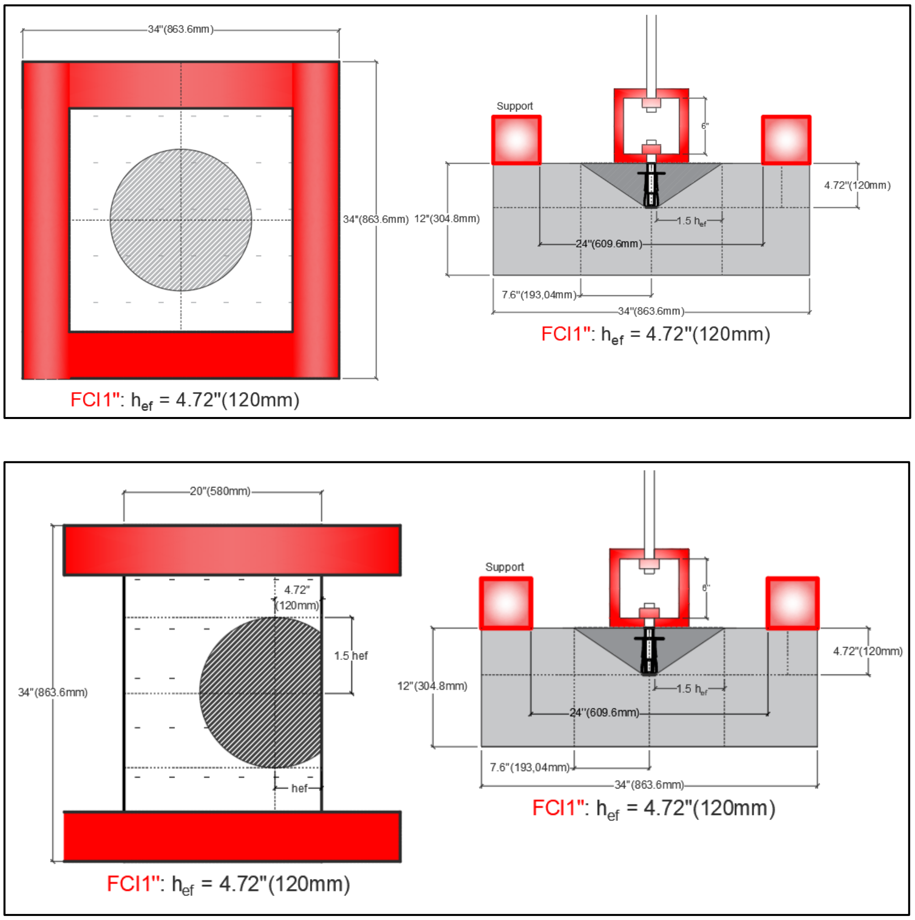

Figure 16. a) The schematic view of the pull-out tension tests: **Center**; **b)** The schematic view of the pull-out tension tests: **Edge**

6.3.2 Shear Test

In the shear test, a hydraulic jack with a 100-kip load capacity was used to load the specimens in shear. The load cell was attached to the top of the hydraulic jack to measure the applied force. The load was increased in accordance with ASTM. E488M – 22 until the failure of the specimen. The experimental setup for evaluating FCI capacity in tension is shown in **Figure 17** and **Figure 19**.

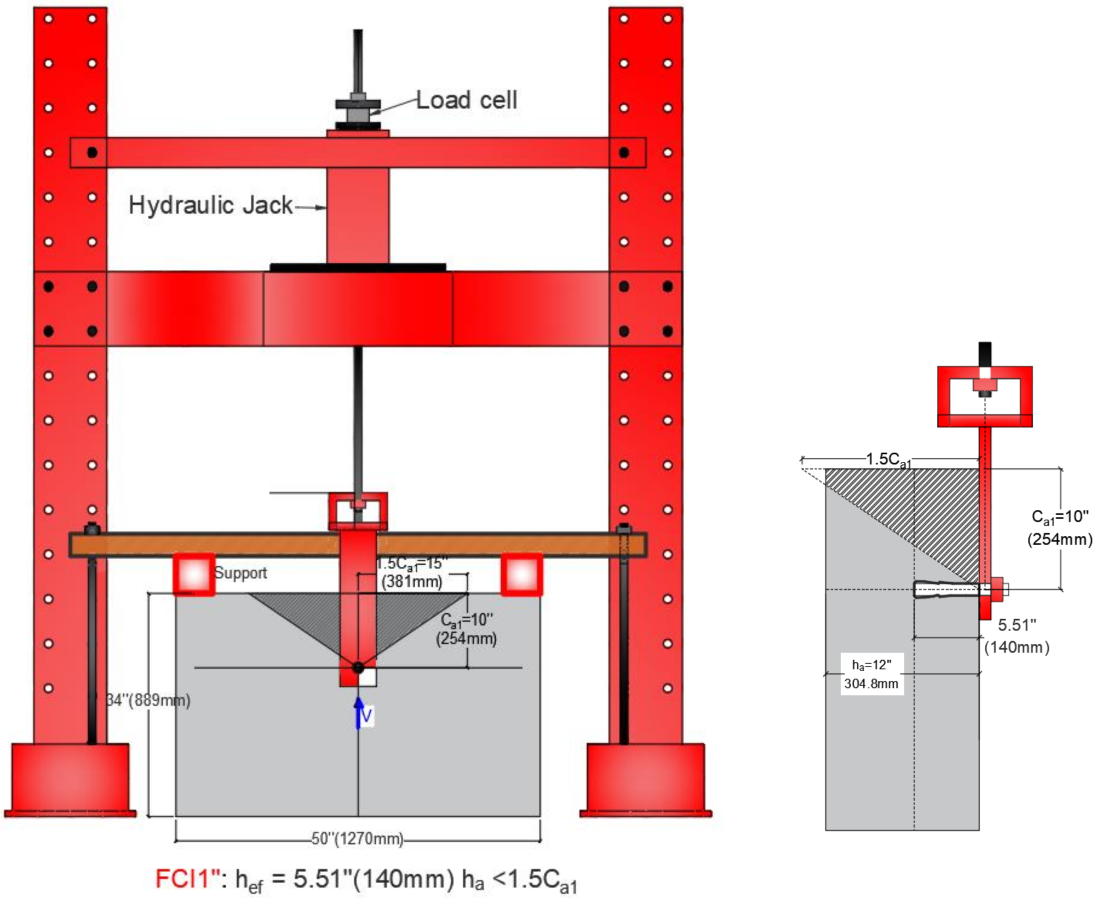

Figure 17. Planned experimental setup for shear tests (including boundary conditions, sensor positions, and specimen position).

To prepare the specimens for testing, the first step was to position the specimen below the hydraulic jack and on its supports (**Figure 18(a)**). Centerlines were marked at the proper locations on the floor of the lab using lasers and chalk-lines. Lead pads were used at the points of load application to obtain a smooth interface between the surface of the specimens and the supporting elements (HSS members were used as support elements as shown in **Figure 18(b)**). In addition, the string potentiometer was attached to the steel plate using wax-coated string tied to eye screws that were tightly fastened in wooden blocks that were glued to the face of the specimen using high-strength epoxy weld adhesive (see **Figure 18(b)**). The final experimental setup is shown in **Figure 19**. **Figure 20** shows the schematic view of the pull-out shear test for the two different cases ($h_a<1.5C_{a1}$ and $h_a>1.5C_{a1}$).

Figure 18. a) Positioning of the specimen; **b)** Positioning of the supports and mounting the string potentiometer at the level of the coupler.

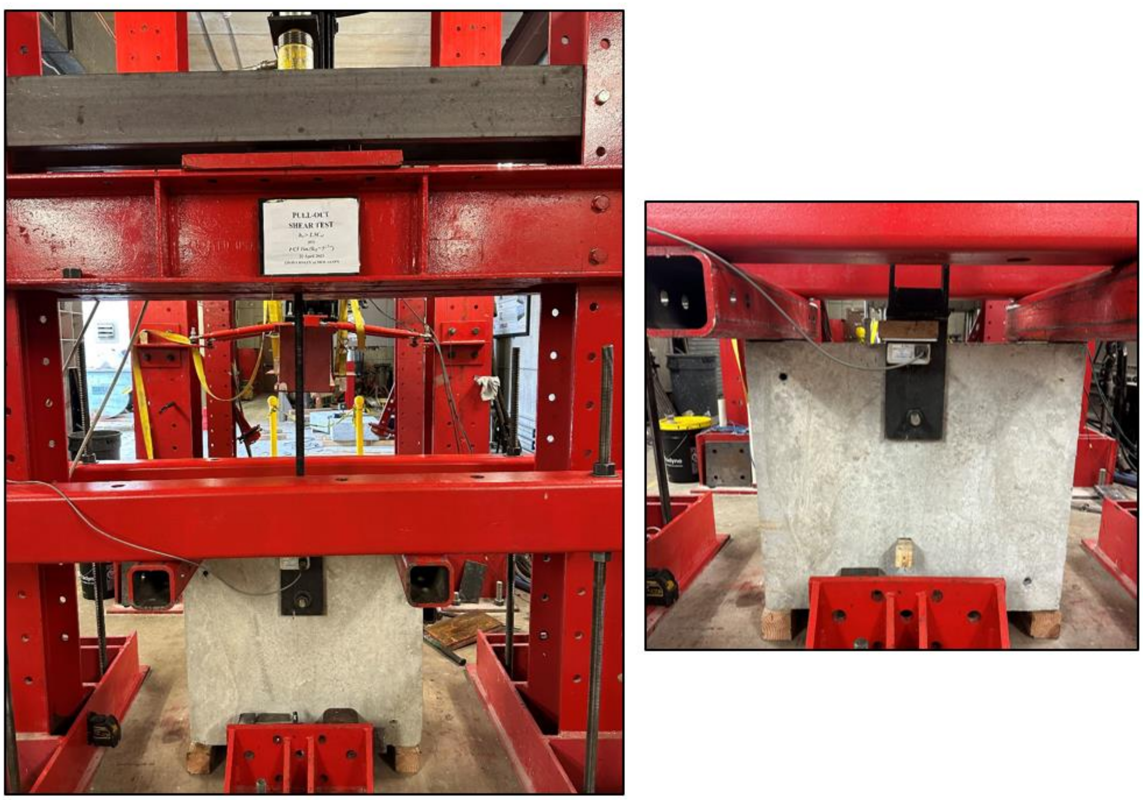

Figure 19. Experimental setup for the shear test.

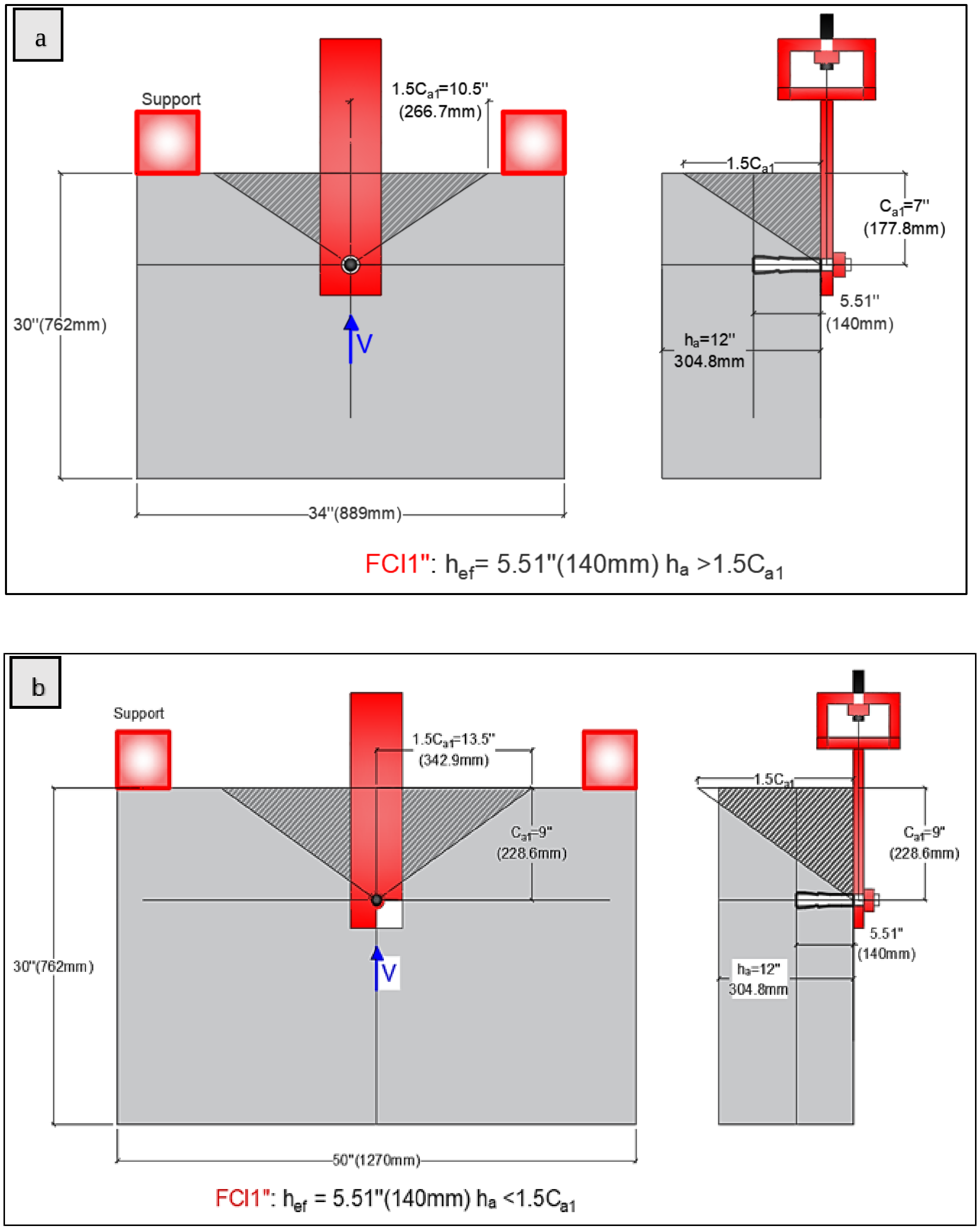

Figure 20. a) The schematic view of the pull-out shear test: $\mathbf{h_a}<\mathbf{\mathit{1.5}C_{a1}}$; **b)** The schematic view of the pull-out shear test: $\mathbf{h_a}>\mathbf{\mathit{1.5}C_{a1}}$.

7 Experimental results

7.1 TENSION TEST

7.1.1 Pull-out Tension Test: Center

In the case of tension tests where the anchors were located at the center of the concrete block, the failure of all the FCI 1/2in. and FCI 5/8in specimens were caused by the concrete breakout cone failure. The same failure occurred for the FCI 1in. with an embedment depth of anchor h_{ef} = 4.72in. (see **Figure 21(a)**). However, a splitting failure occurred for FCI 1in. with an embedment depth of anchor h_{ef} = 5.51in. before reaching the concrete breakout cone (see **Figure 21(b)**) . The detailed results of the tension tests with anchors located in the center are presented in **Appendix A**. The summarized results of the maximum load, the average load for all repetitions of each specimen type, and the ACI prediction (based on equations presented in **Section 5**), are shown in **Table 21**. The experimental results versus the prediction equation of the tension tests where the anchor is located in the center (FCI 1", FCI 2", FCI 3") are presented in **Figure 22**.

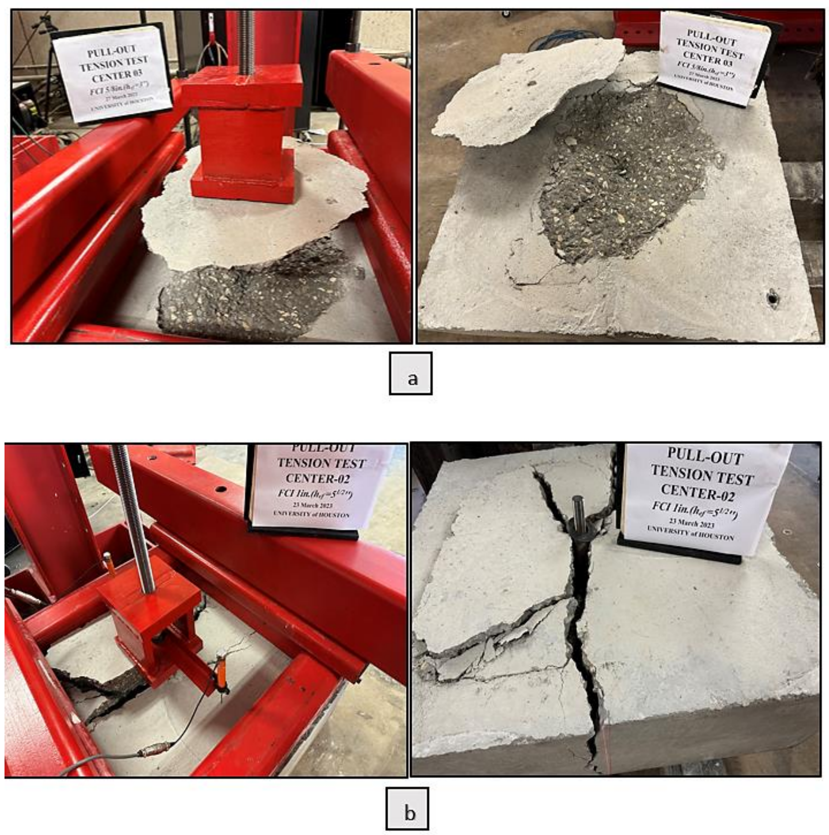

Figure 21. Failure mode (center): **a)** concrete breakout cone failure and **b)** splitting failure.

Table 21. Results of the maximum load, the average load for all repetitions of each specimen type, and the design capacity of the FCI insert (center).

Insert Type	Embedment depth of anchor	Test #	Failure Load (kips)	F_{av} (kips)	*St.dev* (kips)	ACI318-19 (kips)	Failure mode	Insert bottom part broke	FCI Concrete mix
FCI 1"	5.51	1	*26.75*	***24.58***	*1.74*	*20.8*	Splitting + Cone breakout	Yes	*1*
		2	*22.5*				Splitting + Cone breakout	Yes	
		3	*24.5*				Splitting	Yes	
	4.72	1	19.9	***20.57***	*0.57*	*15.37*	Cone breakout	No	*2*
		2D*	21.3				Cone breakout	Yes	
		3	20.5				Cone breakout	No	
FCI 5/8"	3.37	1	10.3	***10.14***	*0.13*	*9.96*	Cone breakout	No	*1*
		2	9.99				Cone breakout	No	
		3	10.14				Cone breakout	No	
	2.97	1	8.3	***8.92***	*0.84*	*8.24*	Cone breakout	No	*1*
		2	10.1				Cone breakout	No	
		3	8.35				Cone breakout	No	
FCI 1/2"	3.11	1	9.7	***8.81***	*0.64*	*8.11*	Cone breakout	Yes	*2*
		2	8.5				Cone breakout	Yes	
		3	8.23				Cone breakout	Yes	
	2.34	1	5.85	***5.92***	*0.33*	*5.30*	Cone breakout	Yes	*2*
		2	5.56				Cone breakout	No	
		3	6.35				Cone breakout	No	

* Specimen damaged at the edge

For all the FCI insert types, the ACI predictions for the failure load are lower than the experimental failure loads (the prediction equation yields values between 75% and 98% of the experimental test values). Hence, one may conclude that the experimental results provide a satisfactory agreement with the ACI equation for the concrete breakout strength of anchors in tension (center).

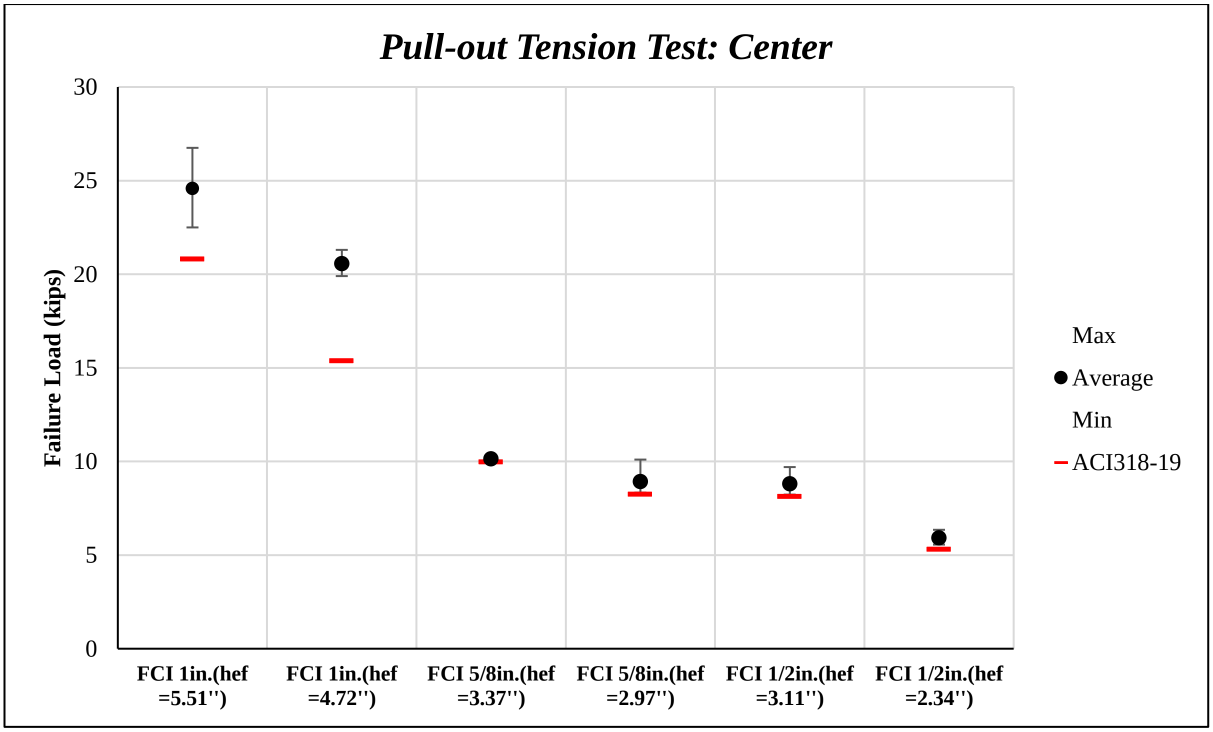

Figure 22. The ACI prediction versus experimental result for FCI 1in., FCI 5/8in., FCI 1/2in. (center).

To obtain results that avoid the splitting failure of the FCI 1" with 5.51in. anchor depth a total of three additional specimens with adjusted dimensions were fabricated and tested at University of Houston laboratory. Furthermore, two additional specimens for FCI 4.72 in. where fabricated and tested to replace the main specimens which were damaged during transportation from the precast plant to the laboratory. For all additional tests, the summarized results of the maximum load, the average load for all repetitions of each specimen type, and the ACI prediction (based on equations presented in **Section 5**) are shown in **Table 22**.

Figure 23 shows the failure of the FCI 1in. with specimens thickness $h > 3\ h_{ef}$. The failure was caused by the concrete breakout cone unlike the first specimens with thickness $h < 3\ h_{ef}$ where the failure was controlled by mixed-mode concrete cone and splitting failure. These results show that increasing member thickness leads to transition of the failure mode from mixed-mode concrete cone and splitting to pure concrete breakout cone failure as well as an increase in the failure load. Increasing member thickness also leads to an increase in the concrete capacity which gives higher concrete breakout strength. The experimental results versus the prediction equation of the additional specimens (FCI 1" with 5.51in. anchor depth) are presented in **Figure 24**.

Table 22. The results of the additional specimens.

Insert Type	Embedment depth of anchor	Test #	Failure Load (kips)	F_{av} (kips)	*St.dev* (kips)	ACI318-19 (kips)	Failure mode	Insert bottom part broke	FCI Concrete mix
FCI 1"	5.51	1	*29.50*	***32.03***	*1.79*	*20.8*	Splitting + Cone breakout	No	*6*
		2	*33.40*				Splitting + Cone breakout	No	
		3	*33.20*				Splitting	No	
	4.72	1	*25.00*	***25.25***	*0.25*	16.51	Cone breakout	No	*6*
		2	*25.58*				Cone breakout	No	*6*

Figure 23. Failure mode of the FCI 1in. (center) with specimen thickness *3* h_{ef}.

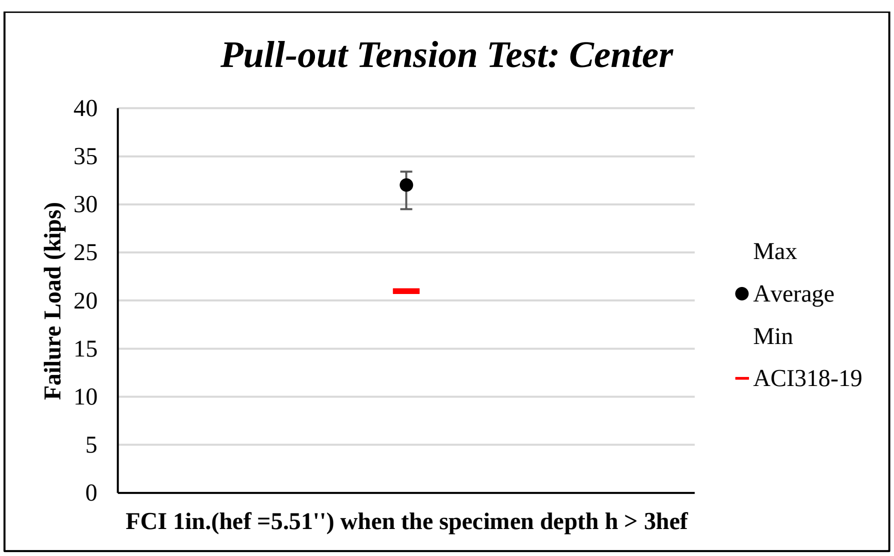

Figure 24. The ACI prediction versus experimental result for FCI 1in. (center) with specimen thickness $h > 3\ h_{ef}$.

7.1.2 Pull out Tension Test: Edge

In the case of tension tests where the anchors were located at the edge of the concrete block, the failure of the FCI 1/2in. and FCI 5/8in specimens were caused by concrete breakout cone failure (see **Figure 25(a)**). However, a splitting failure occurred for all the FCI 1in. before reaching the concrete breakout cone failure (see **Figure 25(b)**). The detailed results of the tension tests where the anchors were located in the edge are presented in **Appendix B**. The summarized results of the maximum load, the average load for all repetitions of each specimen type, and the ACI prediction (based on equations presented in **Section 5**) are shown in **Table 23**. The experimental results versus the prediction equation of the tension tests where the anchor is located on the edge (FCI 1", FCI 2", FCI 3") are presented in **Figure 26**.

During the test of the 1st specimen of FCI 1/2" with 2.34in. depth, the RT experienced an issue with the controller that caused loss of the data for this test. As a result, the average for this case was calculated from the two remaining tests.

Figure 25. Failure mode (edge): **a)** concrete breakout cone failure and **b)** splitting failure.

Table 23. Results of the maximum load, the average load for all repetitions of each specimen type, and the design capacity of the FCI insert (edge).

Insert Type	Embedment depth of anchor	Test #	Failure Load (kips)	F_{av} (kips)	*St.dev* (kips)	ACI318-19 (kips)	Failure mode	Insert bottom part broke	FCI Concrete mix
FCI 1"	5.51	1	14.3	***15.13***	*0.91*	*14.72*	Splitting	No	*4*
		2	14.7				Splitting	No	
		3	16.4				Splitting	No	
	4.72	1	16.03	***15.34***	*0.50*	*11.67*	Cone breakout	No	*4*
		2	15.13				Cone breakout	No	
		3	14.87				Cone breakout	No	
FCI 5/8"	3.37	1	7.94	***7.94***	*0.07*	*6.95*	Cone breakout	No	*5*
		2	8.03				Cone breakout	No	
		3	7.85				Cone breakout	No	
	2.97	1	6.78	***6.77***	*0.30*	*5.75*	Cone breakout	No	*5*
		2	7.13				Cone breakout	No	
		3	6.4				Cone breakout	No	
FCI 1/2"	3.11	1	7.64	***8.28***	*0.54*	*6.24*	Cone breakout	Yes	*5*
		2	8.23				Cone breakout	No	
		3	8.97				Cone breakout	No	
	2.34	1	*	***5.94***	*0.37*	*4.07*	Cone breakout	Yes	*5*
		2	6.31				Cone breakout	No	
		3	5.56				Cone breakout	No	

*Data lost due to a software issue

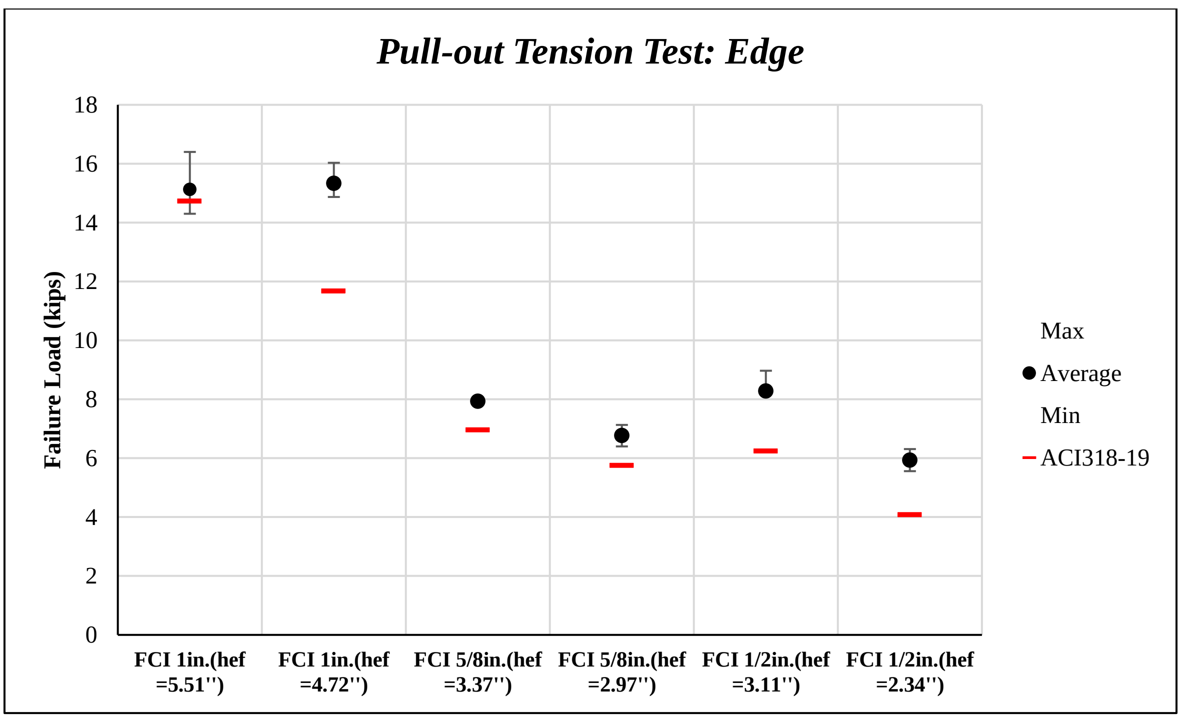

Figure 26. The ACI prediction versus experimental results for FCI 1in., FCI 5/8in., FCI 1/2in. (edge).

Similar to the pull-out tension tests in the center, all the FCI insert types resulted in ACI predicted failure loads lower than the experimental failure loads (the prediction equation yielded values between 69% and 97% of the experimental results). Thus, the experimental results for the edge tests also provide a satisfactory agreement with the ACI equation for the concrete breakout strength.

7.2 SHEAR TEST

7.2.1 Pull-out Shear Test: ha >1.5C_{a1}

In the case of shear tests where *ha >1.5*C_{a1}, the failure of all the FCI 1in specimens was caused by concrete breakout cone failure (see **Figure 27(a)**). However, two specimens had, in addition to the inclined crack on the top surface, a vertical crack along the depth of the specimen (see **Figure 27(b)**). Similar failures have been observed in the work that has been done by Tamon Ueda et al.1990 where the vertical crack was considered to be a flexural crack. The researchers behind this study, therefore, added a third reaction beam in the longitudinal direction to prevent the flexural cracks (see **Figure 28(a)**). Jong-Han Lee et al.2018 studied the shear capacity of cast-in headed anchors in steel fiber-reinforced concrete, and, for the anchors in plain concrete, there was an inclined crack on both sides of the top surface followed by a vertical crack along the depth of the anchor (see **Figure 28(b)**).

Figure 27. Failure mode for FCI 1in. (*ha >1.5*C_{a1},): **a)** concrete breakout cone failure and **b)** vertical crack along the depth of the specimen.

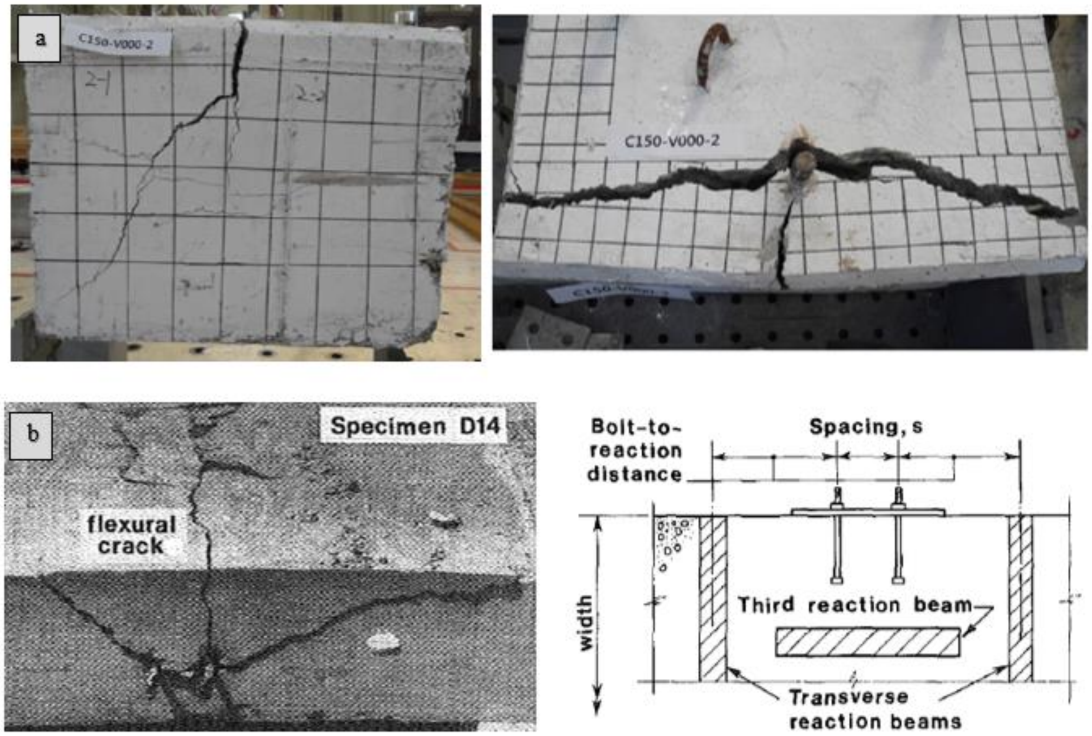

Figure 28. Failure mode for: **(a)** Shear capacity of cast-in headed anchors by J.Han Lee et al.2018. **(b)** Anchor bolts under shear by Tamon Ueda et al.1990.

A unique behavior of the FCI that was observed in the shear tests (and not the tension tests) is that the FCI experienced high stresses at the top part of the insert which caused the FCI to fracture as shown in **Figure 29**. This occurred as a result of the FCI inserts not being fully threaded along their length thereby allowing for contact of the anchor with the un-threaded part of the insert under shear loading coditions (see **Figure 30**). For tests with FCI 1/2in. and FCI 5/8in, the failure mode of all the specimens was the concrete breakout cone failure (see **Figure 31**); however, all of the FCI inserts failed at the top part. The concrete breakout cone failure in **Figure 31** is similar to the predicted failure according to ACI in the case of $h_a < 1.5C_{a1}$ (see **Figure 3**).

Figure 29. FCI insert fracture at the top.

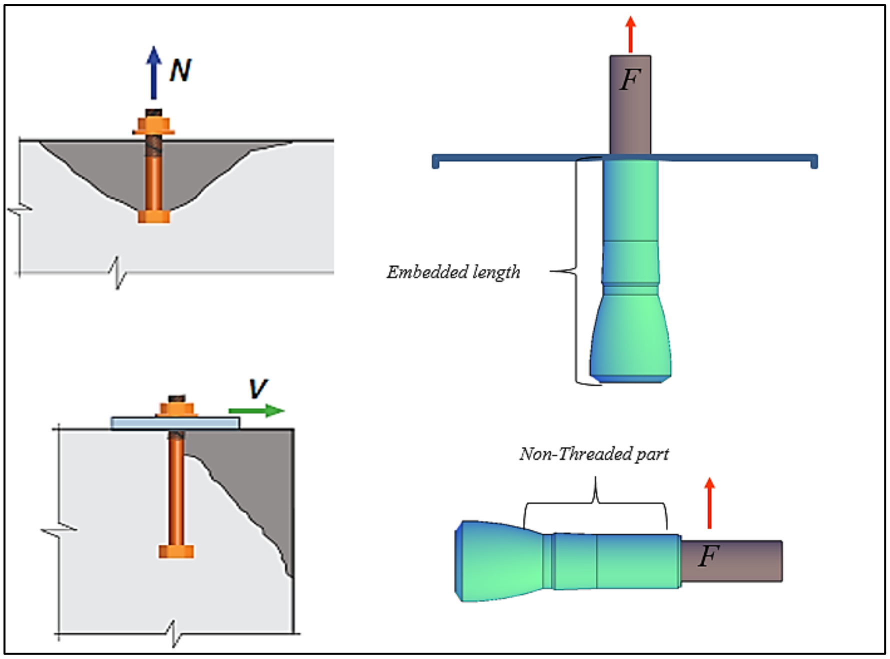

Figure 30. (a) Embedded length for the tension tests; **(b)** Non-threaded part in the shear tests.

The detailed results of of shear tests when $h_a > 1.5C_{a1}$ are presented in **Appendix C**. The summarized results of the maximum load, the average load for all repetitions of each specimen type, and the ACI prediction (based on equations presented in **Section 5**) are shown in **Table 24**. The experimental results versus the prediction equation of the shear tests where $h_a > 1.5C_{a1}$ (FCI 1", FCI 2", FCI 3") are presented in **Figure 32**.

Figure 31. Failure mode of **(a)** FCI 5/8in. and **(b)** FCI 1/2in.

Table 24. Results of the maximum load, the average load for all repetitions of each specimen type, and the design capacity of the FCI insert ($h_a > 1.5C_{a1}$).

Insert Type	Embedment depth of anchor	Test #	Failure Load (kips)	F_{av} (kips)	*St.dev* (kips)	ACI318-19 (kips)	Failure mode	Insert Top part broke	FCI Concrete mix
FCI 1"	5.51	1	17.80	***17.07***	*0.66*	10.54	Cone breakout + Vertical crack along the depth	yes	*3*
		2	17.20				Cone breakout	yes	
		3	16.20				Cone breakout	yes	
	4.72	1	17.40	***17.53***	*0.85*	10.54	Cone breakout + Vertical crack along the depth	yes	*3*
		2	18.6				Cone breakout	yes	
		3	16.6				Cone breakout	yes	
FCI 5/8"	3.37	1	8.10	***8.37***	*0.6*	6.36	Cone breakout	yes	*6*
		2	9.20				Cone breakout	yes	
		3	7.80				Cone breakout	yes	
	2.97	1	9.00	***8.5***	*0.37*	6.36	Cone breakout	yes	*6*
		2	8.10				Cone breakout	yes	
		3	8.40				Cone breakout	yes	
FCI 1/2"	3.11	1	8.50	***8.42***	*0.23*	5.69	Cone breakout	yes	*6*
		2	8.65				Cone breakout	yes	
		3	8.10				Cone breakout	yes	
	2.34	1	7.50	***8.13***	*0.46*	5.69	Cone breakout	yes	*6*
		2	8.30				Cone breakout	yes	
		3	8.60				Cone breakout	yes	

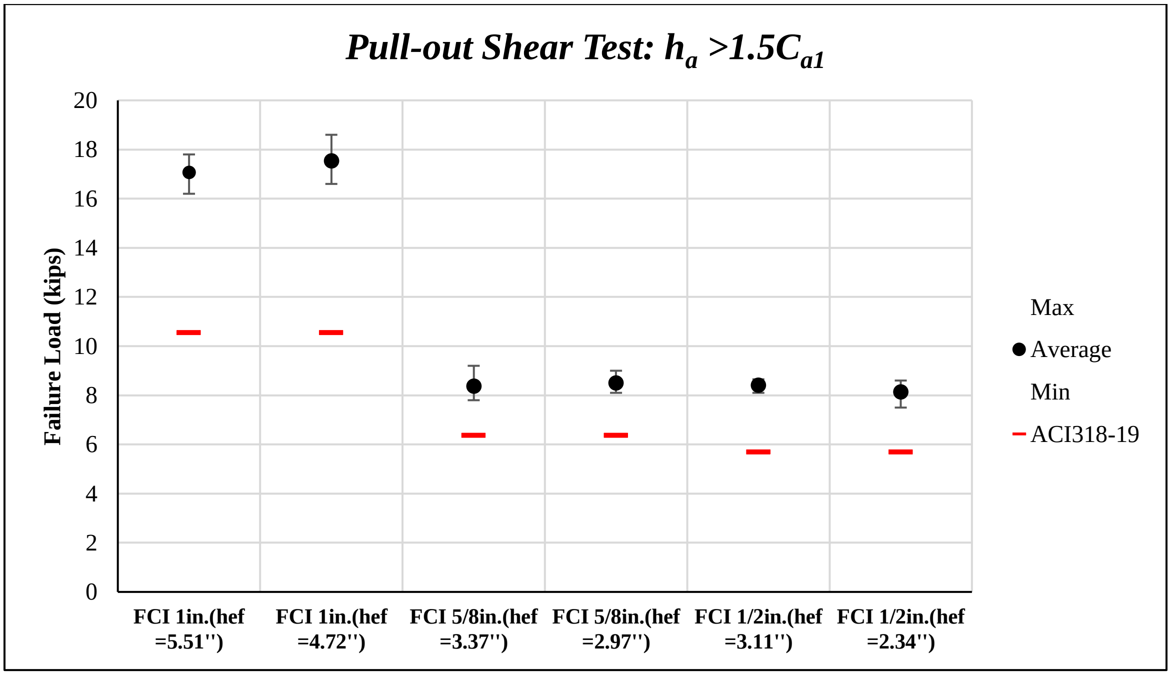

Figure 32. The ACI prediction versus experimental result for FCI 1in., FCI 5/8in., FCI 1/2in. ($h_a > 1.5C_{a1}$).

As shown in **Figure 32**, the ACI predictions resulted in lower failure loads for all the FCI insert types compared to the experimental failure loads (the prediction equation yielded values between 60% and 76% of the experimental results). Thus, it may be concluded that the experimental results provide a satisfactory agreement with the ACI equation for the concrete breakout strength of anchors in shear tests in the case of $h_a > 1.5C_{a1}$.

7.2.2 Pull-out Shear Test: $h_a < 1.5C_{a1}$

In the case of shear tests where $h_a < 1.5C_{a1}$, the failure mode of all the FCI 1in. specimens was the concrete breakout cone failure (see **Figure 33**). A similar failure occurred for FCI 5/8in. (see **Figure 34**) except for one specimen that exhibited an additional vertical crack along the depth of the specimen (see **Figure 35**). The general failure is similar to the predicted failure defined by ACI and shown in **Figure 3**. For tests with the FCI 1/2in., the steel strength was close to the concrete breakout strength of the FCI insert in shear. As a result, the steel failure occured before reaching the concrete breakout strength for FCI 1/2in. with depth of anchor h_{ef} = 3.11in. (see **Figure 36(a)**) For the FCI 1/2in. with depth of anchor h_{ef} = 2.34in. the failure was controlled by mixed-mode concrete cone and anchor bending (see **Figure 36(b)**).

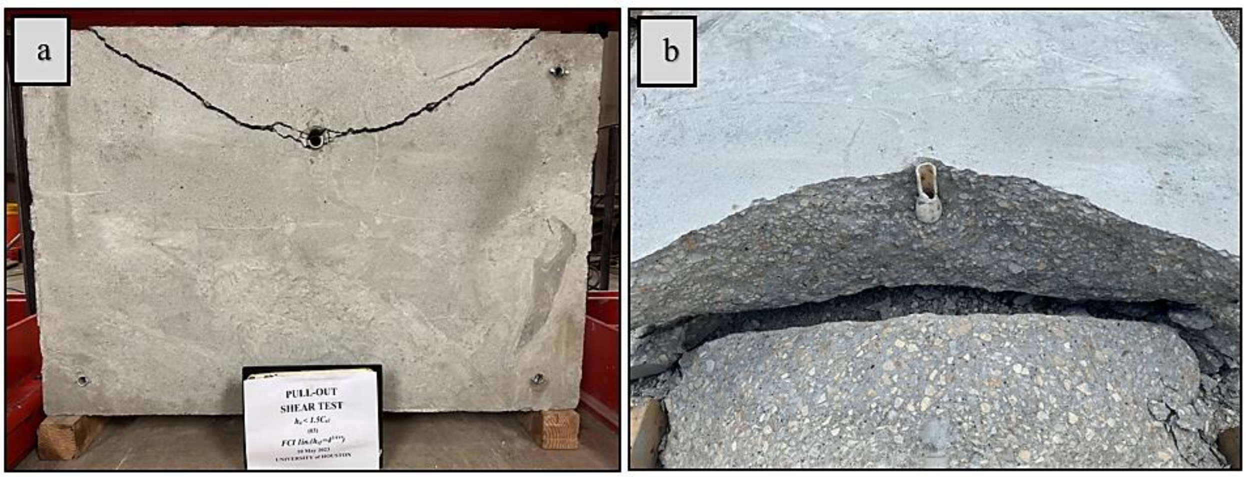

Figure 33. Failure mode for FCI 1in. (*ha* $< 1.5C_{a1}$,): concrete breakout cone failure.

Figure 34. Failure mode for FCI 5/8in. ($h_a < 1.5C_{a1}$,): concrete breakout cone failure.

Figure 35. Failure mode for FCI 5/8in. ($h_a < 1.5C_{a1}$,): concrete breakout cone failure + vertical crack along the depth of the specimen.

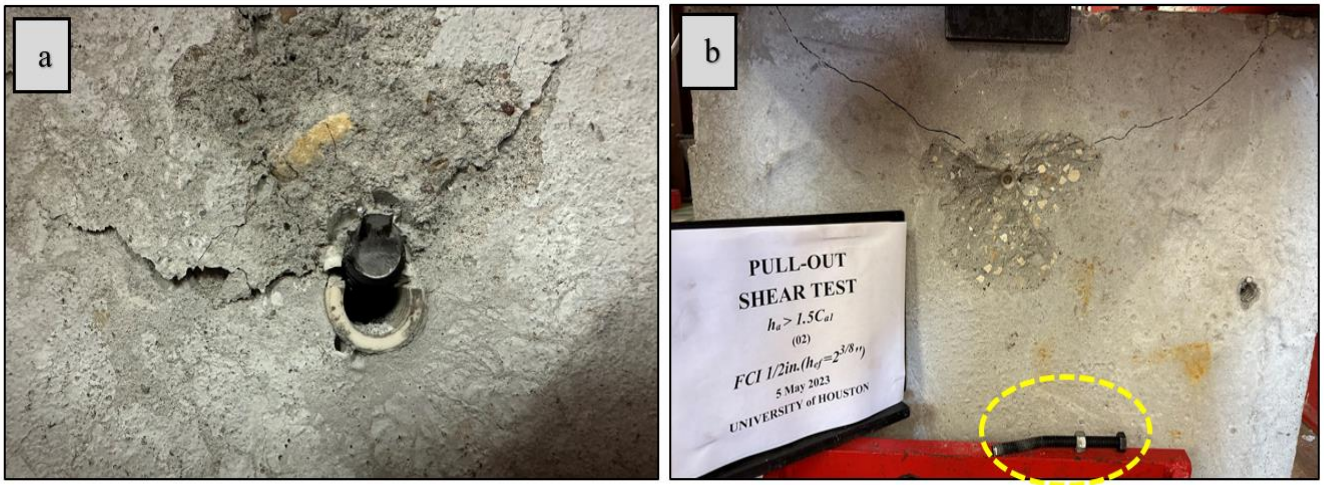

Figure 36. Failure mode for FCI 1/2in. (*ha* $<1.5C_{a1}$,): **(a)** 3.11in. anchor failure **(a)** 2.34in. anchor failure.

Similar to the shear tests of $h_a > 1.5C_{a1}$, the FCI experienced high stresses at the top part of the insert which caused fracture of the FCI as shown in **Figure 37**.

Figure 37. FCI insert fracture at the top.

The detailed results of of shear tests when *ha* $<1.5C_{a1}$ are presented in **Appendix D**. The summarized results of the maximum load, the average load for all repetitions of each specimen type, and the ACI prediction (based on equations presented in **Section 5**) are shown in **Table 25**. The experimental results versus the prediction equation of the shear tests where *ha* $<1.5C_{a1}$ (FCI 1", FCI 2", FCI 3") are presented in **Figure 38**.

Table 25. Results of the maximum load, the average load for all repetitions of each specimen type, and the design capacity of the FCI insert ($h_a < 1.5C_{a1}$).

Insert Type	Embedment depth of anchor	Test #	Failure Load (kips)	F_{av} (kips)	*St.dev* (kips)	ACI318-19 (kips)	Failure mode	Insert Top part broke	FCI Concrete mix
FCI 1"	5.51	1	28.00	***28.73***	*0.71*	16.04	Cone breakout	yes	*4*
		2	29.70				Cone breakout	yes	
		3	28.50				Cone breakout	yes	
	4.72	1	26.10	***27.10***	*0.96*	16.04	Cone breakout	yes	*4*
		2	26.80				Cone breakout	yes	
		3	28.40				Cone breakout	yes	
FCI 5/8"	3.37	1	14.40	***13.65***	*0.53*	10.14	Cone breakout	yes	*5*
		2	13.30				Cone breakout	yes	
		3	13.26				Cone breakout+ Vertical crack along the depth	yes	
	2.97	1	13.50	***12.97***	*0.38*	10.14	Cone breakout	yes	*5*
		2	12.77				Cone breakout	yes	
		3	12.63				Cone breakout	yes	
FCI 1/2"	3.11	1	10.13	***10.61***	*1.39*	9.07	Anchor failure	yes	*5*
		2	9.20				Anchor failure	yes	
		3	12.50				Anchor failure	yes	
	2.34	1	12.00	***11.37***	*1.58*	9.07	FCI failure + Anchor failure	yes	*5*
		2	12.90				FCI failure + Anchor failure	yes	
		3	9.20				Cone breakout + Anchor failure	yes	

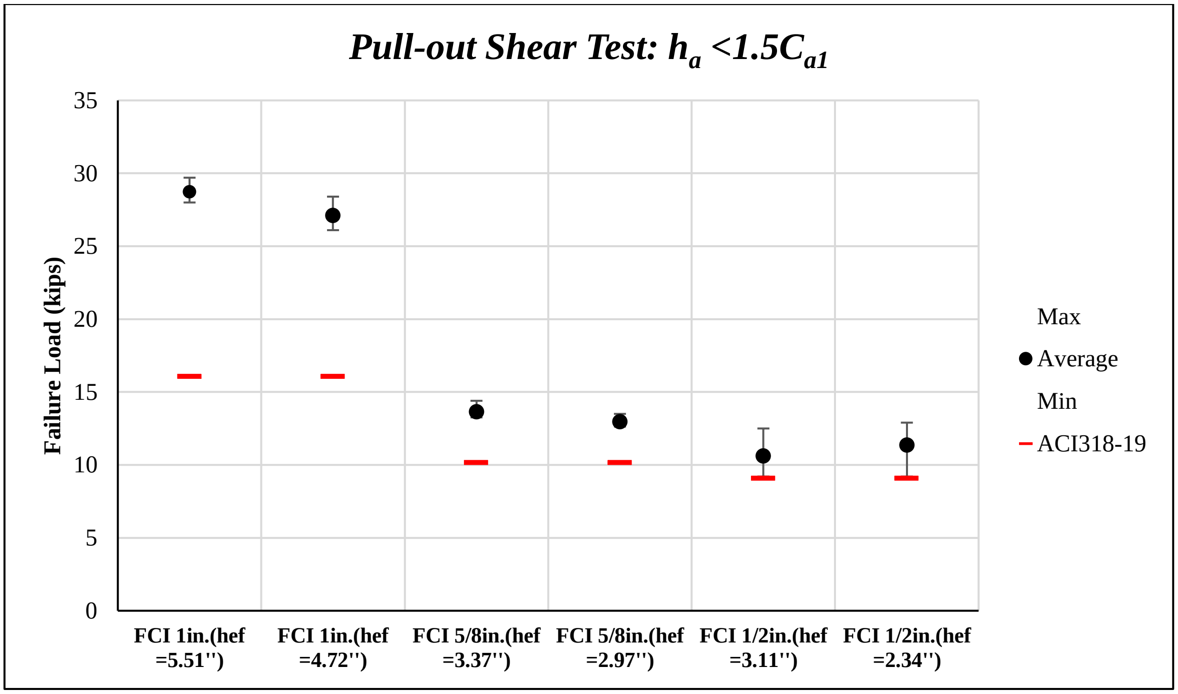

Figure 38. The ACI prediction versus experimental result for FCI 1in., FCI 5/8in., FCI 1/2in.(*ha <1.5Ca1*).

For the 1in. and 5/8 in. FCI inserts, the predictions for the failure loads using the ACI equation are lower than the experimental failure loads (the prediction equation yielded values between 56% and 80% of the experimental results). Therefore,it may be concluded that the experimental results provide a satisfactory agreement with the ACI equation for the concrete breakout strength in the case of $h_a < 1.5C_{a1}$. For the FCI 1/2in., the steel strength was close to the concrete breakout strength of the FCI insert in shear. As a result, the steel failure occurred before the specimen could reach the concrete breakout strength for FCI 1/2in. However, the failure load was above the ACI prediction of the concrete breakout strength of anchors in shear.

The overall testing results for both tension and shear are shown in **Figure 39**. The results from all of the 76 experimental tests are above the ACI prediction. Thus, the results from the experimental program within the scope of this work show that the use of the ACI equation will provide a relatively conservative estimation of the concrete capacity of the FCI insert.

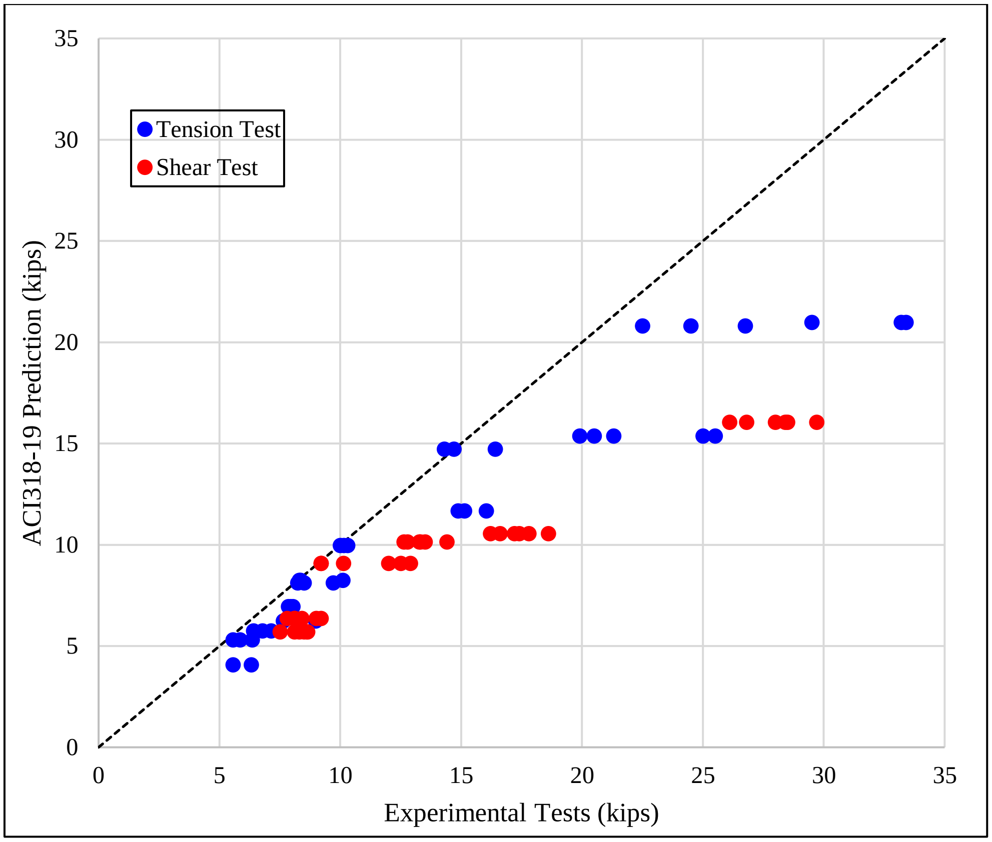

Figure 39. The overall testing results for both tension and shear tests for FCI 1in., FCI 5/8in., FCI 1/2in.

8 CONCLUDING REMARKS

The overall objective of this research project was to evaluate the strength FCI inserts under tension and shear tests. The FCI was tested under different monotonic loading conditions based on the US standard testing protocol. The experimental program included tension tests for anchors located in the center and edge of concrete blocks as well as shear tests for two different cases. The test specimens were all designed to induce concrete failure and insert failure. The main conclusions derived from the results obtained from this investigation are summarized as follows. Note that the test results are based on average results and without including any statistical analysis.

- For all the FCI insert types tested in the pull-out tension tests (with anchors located at the center), the ACI predictions of the failure load are lower than the experimental failure loads (the prediction equation yielded results between 75% and 98% of the experimental results).
- Similarly, all of the FCI insert types for pull-out tension tests with anchors located at the edge, the ACI prediction for the failure load was lower than the experimental tests (the prediction equation yielded values between 69% and 97% of the experimental results).
- Based on the results of all pull-out tension tests, it may be concluded that the experimental results for both the center and the edge tests provide a satisfactory results when comparing ACI equation for concrete breakout strength.
- For shear tests with $h_a > 1.5C_{a1}$, the ACI predictions resulted in lower failure loads for all the FCI insert types compared to the experimental failure loads (the prediction equation yielded values between 60% and 76% of the experimental results).
- In the case of the shear test ($ha < 1.5C_{a1}$), the predictions of the failure loads using the ACI equation are lower than the experimental tests for the case of 1in. and 5/8 in. FCI inserts. (the prediction equation is between 56% and 80% of the experimental results). Therefore, it may be concluded that the experimental results provide a satisfactory results based on the ACI equation for the concrete breakout strength in the case of $h_a < 1.5C_{a1}$.
- For the FCI 1/2in., the steel strength of the anchor was close to the concrete breakout strength of the FCI insert in shear, and the steel failure occurred before reaching the concrete breakout strength for FCI 1/2in. However, the failure load was above the ACI prediction of the concrete breakout strength of the anchor in shear.
- The results from all of the 76 experimental tests exceeded the ACI prediction for concrete cone . Thus, the results from the experimental program within the scope of this work show that the use of the ACI equation will provide a relatively conservative estimation of the concrete capacity of the FCI insert.
- The general failure for the majority of the tested specimens are similar to the predicted failures defined by ACI (see **Figure 3**).

9 Acknowledgements

The Experimental study included in this report was suppoted by Japan Life Co., Ltd. Their financial support is gratefully acknowledged. Special thanks and appreciations go to Mr. Jay M. Cariveau of Legacy Precast, LLC and Dr. Larbi Sennour of CEG International, Inc for facilitating and assisting in the fabrication of test specimens as well as Mr. Scott Smart, lab specialist at the University of Houston's Structural Laboratory for his contribution in fabrication and testing of test specimens.

10 References

ACI 355.2, 2007. Qualification of Post-installed Mechanical Anchors in Concrete (ACI 355.2-07) and Commentary. American Concrete Institute (ACI), Farmington Hills, MI.

ACI Committee 318. ACI 318-19 (2019). Building Code Requirements for Structural Concrete and Commentary; .

Al-Taan, S., Al-Jaffal, A., and Mohammed, A. A. (2012). "Breakout capacity of headed anchors in steel fibre normal and high strength concrete." Asian Journal of Applied Sciences, pp. 485-496, DOI: 10.3923/ajaps.2012.485.496.

ASTM E 488-96 reapproved (2003). Standard Test Methods for Strength of Anchors in Concrete and Masonry Elements, American Society for Testing and Materials, West Conshohocken, PA, US.

ASTM C900 (2020). Standard Test Methods for Pullout Strength of Hardened Concrete, American Society for Testing and Materials, West Conshohocken, PA, US.

Chen, Z. (2021, December). A review of current research progress on tensile behavior of expansion anchors in concrete. In *Structures* (Vol. 34, pp. 2276-2287). Elsevier.

Cook, R. A., Kunz, J., Fuchs, W., & Konz, R. C. (1998). Behavior and design of single adhesive anchors under tensile load in uncracked concrete. *Structural Journal*, *95*(1), 9-26.

Cook, R. A., & Klingner, R. E. (1992). Ductile multiple-anchor steel-to-concrete connections. *Journal of structural engineering*, *118*(6), 1645-1665.

Delhomme, F., & Debicki, G. (2010). Numerical modelling of anchor bolts under pull-out and relaxation tests. *Construction and Building Materials*, *24*(7), 1232-1238.

Delhomme, F., Pallud, B., & Rouane, N. (2018). Tightening torque influence on pull-out behavior of post-installed expansion anchors. *KSCE Journal of Civil Engineering*, *22*(10), 3931-3939.

Eligehausen, R., Mallee, R., and Solva, J. F. (2006). Anchorage in Concrete Construction, Ernst & Sohn, Berlin, Germany.

Eligehausen, R., & Balogh, T. (1995). Behavior of fasteners loaded in tension in cracked reinforced concrete. *Structural Journal*, *92*(3), 365-379.

El Sharnouby, M. M., & El Naggar, M. H. (2010). Numerical investigation of the response of expansion anchors used to attach helical pile connectors to concrete foundations. *Canadian Journal of Civil Engineering*, *37*(6), 866-877.

EN 1992-4, Eurocode 2. Design of concrete structures. Design of fastenings for use in concrete. BSI; 2018.

Fushs, W., Eligehausen, R., and Breen, J. E. (1995). "Concrete Capacity Design (CCD) approach for fastening to concrete." ACI Structural Journal, Vol. 92, pp. 73-94.

Furche, J., & Eligehausen, R. (1991). Lateral blow-out failure of headed studs near a free edge.

Ghobarag, A. and Aziz, T. (2004). "Seismic qualification of expansion anchors to Canadian nuclear standards." Nuclear Engineering and Design, Vol. 228, Issues 1-3, pp. 377-392, DOI: 10.1016/j.nucengdes. 2004.01.021.

Goto, Y. (1971, April). Cracks formed in concrete around deformed tension bars. In *Journal Proceedings* (Vol. 68, No. 4, pp. 244-251).

Japan Life Co., Ltd, (2011). FINE CERAMIC INSERT,Technical Data, Japan Life Co., Ltd, Tokyp, Japan.

Karmokar, T., Mohyeddin, A., Lee, J., & Paraskeva, T. (2021). Concrete cone failure of single cast-in anchors under tensile loading–A literature review. *Engineering Structures*, *243*, 112615.

Kim, J. S., Jung, W. Y., Kwon, M. H., & Ju, B. S. (2013). Performance evaluation of the post-installed anchor for sign structure in South Korea. *Construction and Building Materials*, *44*, 496-506.

Lee, J. H., Cho, B., Kim, J. B., Lee, K. J., & Jung, C. Y. (2018). "Shear capacity of cast-in headed anchors in steel fiber-reinforced concrete". *Engineering Structures*, *171*, 421-432.

Mahrenholtz, P., & Eligehausen, R. (2015). "Post-installed concrete anchors in nuclear power plants: Performance and qualification". *Nuclear Engineering and Design*, *287*, 48-56.

Nilforoush, R., Nilsson, M., & Elfgren, L. (2017). Experimental evaluation of tensile behaviour of single cast-in-place anchor bolts in plain and steel fibre-reinforced normal-and high-strength concrete. *Engineering Structures*, *147*, 195-206.

Pallarés, L., & Hajjar, J. F. (2010). "Headed steel stud anchors in composite structures, Part I: Shear". *Journal of Constructional Steel Research*, *66*(2), 198-212.

Pallarés, L., & Hajjar, J. F. (2010). "Headed steel stud anchors in composite structures, Part II: Tension and interaction". *Journal of Constructional Steel Research*, *66*(2), 213-228.

Standards Australia committee, AS 5216:2018: Design of post-installed and cast-in fastenings in concrete. Sai Global; 2018.

Tian, Kaipei, and Joško Ožbolt. "Concrete pry-out failure of single headed stud anchors after fire exposure: Experimental and numerical study." *Engineering Structures* 232 (2021): 111816.

Ueda, T., Kitipornchai, S., & Ling, K. (1990). Experimental investigation of anchor bolts under shear. *Journal of structural engineering*, *116*(4), 910-921.

Appendix A

Pull-out Tension Test

(Center)

Appendix A1.1

Sample:	FCI 1in. (h_{ef} = 5.51in.) - **01**
Mode of failure:	***Splitting + Cone breakout***
Maximum load (kips):	***26.75***
Observation	The insert in the bottom part broke

Figure A1.1 The image of the specimen before failure and after failure.

Appendix A1.2

Sample:	FCI 1in. (h_{ef} = 5.51in.) - **02**
Mode of failure:	***Splitting + Cone breakout***
Maximum load (kips):	***22.5***
Observation	The insert in the bottom part broke

Figure A1.2 The image of the specimen before failure and after failure.

Appendix A1.3

Sample:	FCI 1in. (h_{ef} = 5.51in.) - **03**
Mode of failure:	***Splitting***
Maximum load (kips):	***24.5***
Observation	The insert in the bottom part broke

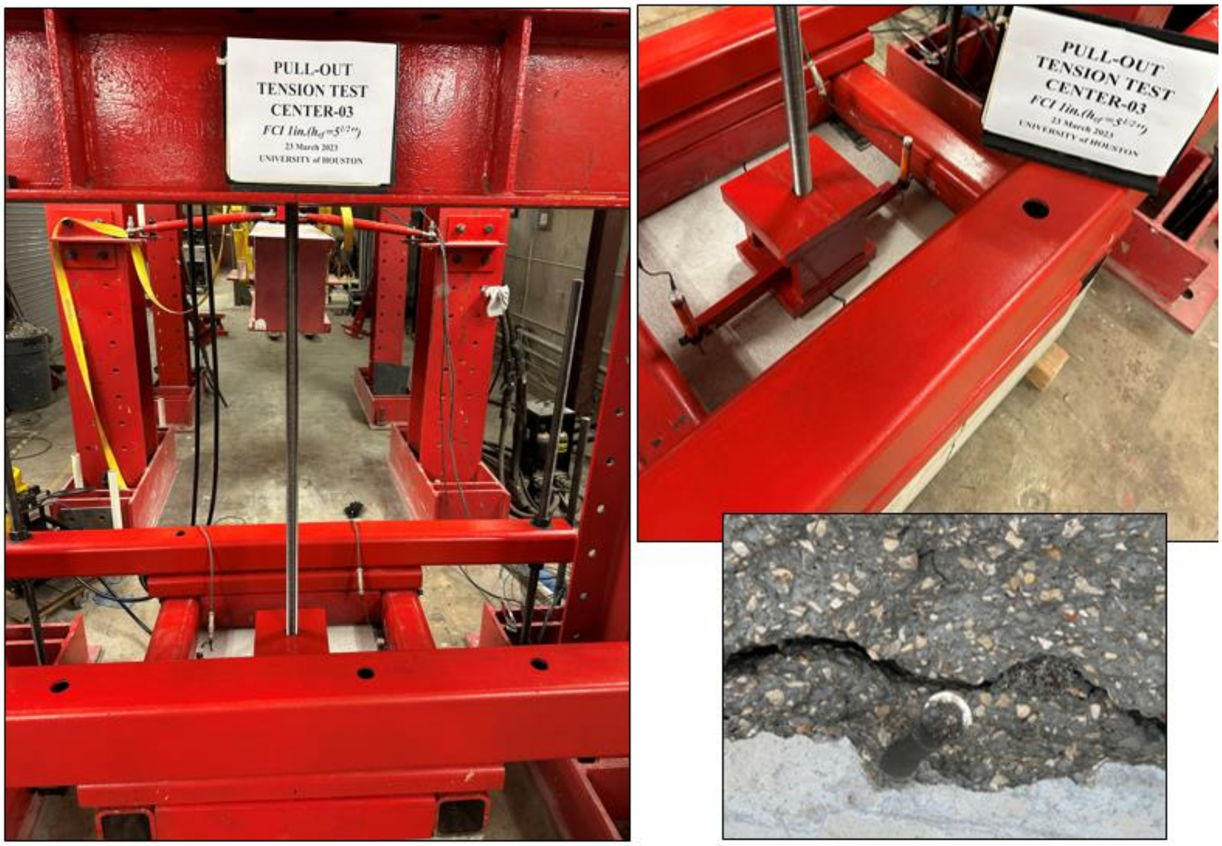

Figure A1.3 The image of the specimen before failure and after failure.

Appendix A2.1

Sample: FCI 1in. (h_{ef} = 4.72in.) - **01**

Mode of failure: ***Cone breakout***

Maximum load (kips): ***19.9***

Observation -

Figure A2.1 The image of the specimen before failure and after failure.

Appendix A2.2

Sample: FCI 1in. (h_{ef} = 4.72in.) - **02**

Mode of failure: ***Cone breakout***

Maximum load (kips): ***21.3***

Observation
- The insert in the bottom part broke
- The specimen damaged at the edge while they were transporting them.

Figure A2.2 The image of the specimen before failure and after failure.

Appendix A2.3

Sample: FCI 1in. (h_{ef} = 4.72in.) - **03**

Mode of failure: ***Cone breakout***

Maximum load (kips): ***20.5***

Observation -

Figure A2.3 The image of the specimen before failure and after failure.

Appendix A3.1

Sample:	FCI 5/8in. (h_{ef} = 3.37in.) - **01**
Mode of failure:	***Cone breakout***
Maximum load (kips):	***10.3***
Observation	-

Figure A3.1 The image of the specimen before failure and after failure.

Appendix A3.2

Sample:	FCI 5/8in. (h_{ef} = 3.37in.) - **02**
Mode of failure:	***Cone breakout***
Maximum load (kips):	***9.99***
Observation	-

Figure A3.2 The image of the specimen before failure and after failure.

Appendix A3.3

Sample:	FCI 5/8in. (h_{ef} = 3.37in.) - **03**
Mode of failure:	***Cone breakout***
Maximum load (kips):	***10.3***
Observation	-

Figure A3.3 The image of the specimen before failure and after failure.

Appendix A4.1

Sample: FCI 5/8in. (h_{ef} = 2.97in.) - **01**
Mode of failure: ***Cone breakout***
Maximum load (kips): ***8.3***
Observation -

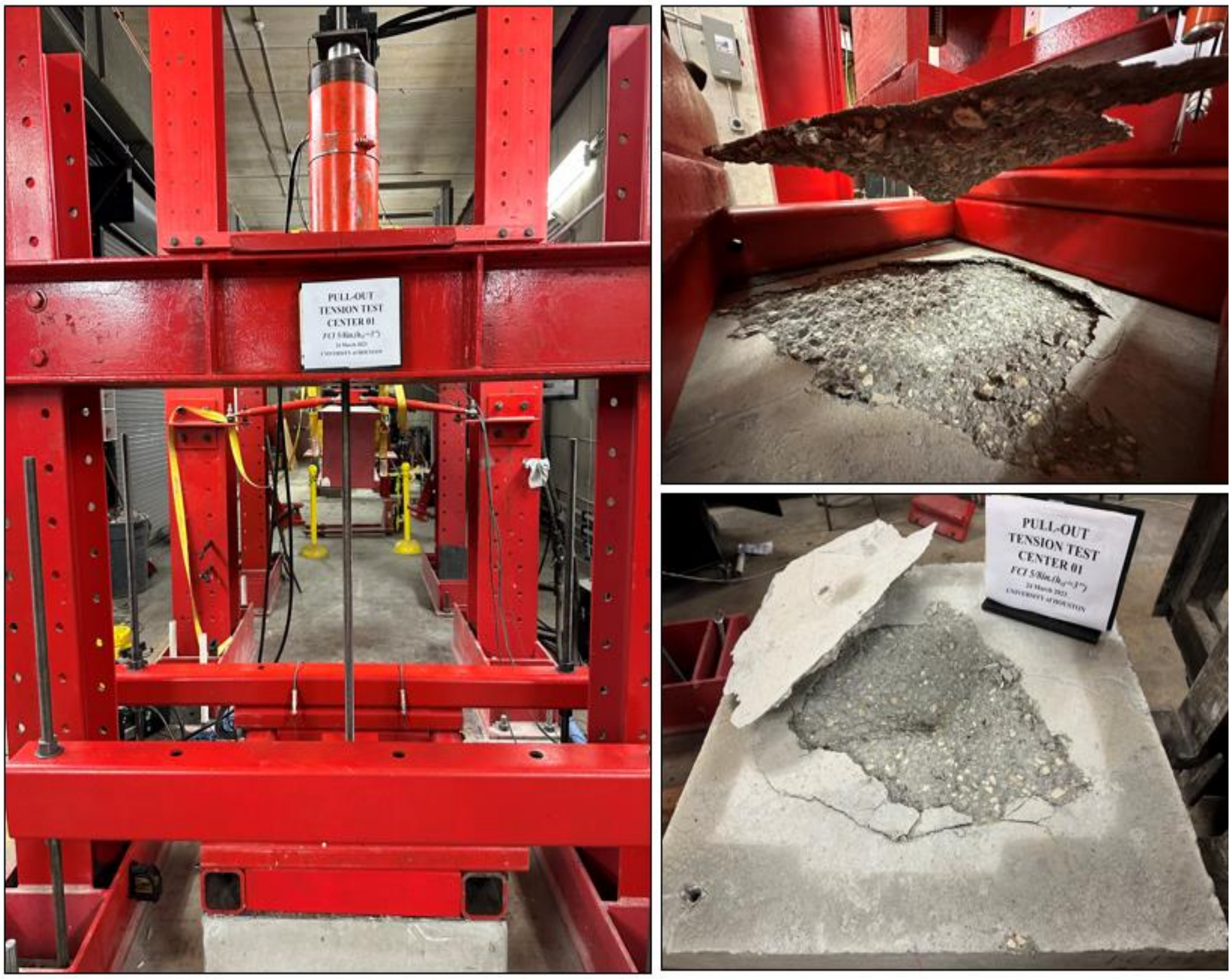

Figure A4.1 The image of the specimen before failure and after failure.

Appendix A4.2

Sample: FCI 5/8in. (h_{ef} = 2.97in.) - **02**

Mode of failure: ***Cone breakout***

Maximum load (kips): ***10.1***

Observation -

Figure A4.2 The image of the specimen before failure and after failure.

Appendix A4.3

Sample: FCI 5/8in. (h_{ef} = 2.97in.) - **03**

Mode of failure: ***Cone breakout***

Maximum load (kips): ***8.35***

Observation -

Figure A4.3 The image of the specimen before failure and after failure.

Appendix A5.1

Sample: FCI 1/2in. (h_{ef} =3.11in.) - **01**

Mode of failure: ***Cone breakout***

Maximum load (kips): ***9.7***

Observation
- The insert in the bottom part broke

Figure A5.1 The image of the specimen before failure and after failure.

Appendix A5.2

Sample:	FCI 1/2in. (h_{ef} =3.11in.) - **02**
Mode of failure:	***Cone breakout***
Maximum load (kips):	***8.5***
Observation	- The insert in the bottom part broke

Figure A5.2 The image of the specimen before failure and after failure.

Appendix A5.3

Sample:	FCI 1/2in. (h_{ef} =3.11in.) - **03**
Mode of failure:	***Cone breakout***
Maximum load (kips):	***8.23***
Observation	- The insert in the bottom part broke

Figure A5.3 The image of the specimen before failure and after failure.

Appendix A6.1

Sample:	FCI 1/2in. (h_{ef} =2.34in.) - **01**
Mode of failure:	***Cone breakout***
Maximum load (kips):	***5.85***
Observation	- The insert in the bottom part broke

Figure A6.1 The image of the specimen before failure and after failure.

Appendix A6.2

Sample:	FCI 1/2in. (h_{ef} =2.34in.) - **02**
Mode of failure:	***Cone breakout***
Maximum load (kips):	***5.56***
Observation	-

Figure A6.2 The image of the specimen before failure and after failure.

Appendix A6.3

Sample: FCI 1/2in. (h_{ef} =2.34in.) - **03**
Mode of failure: ***Cone breakout***
Maximum load (kips): ***6.35***
Observation -

Figure A6.3 The image of the specimen before failure and after failure.

Appendix A7.1

Sample:	FCI 1in. (h_{ef} = 5.51in.) - **01**
Mode of failure:	***Cone breakout***
Maximum load (kips):	***29.5***
Observation	The insert in the top part broke

Figure A7.1 The image of the specimen before failure and after failure.

Appendix A7.2

Sample:	FCI 1in. (h_{ef} = 5.51in.) - **02**
Mode of failure:	***Cone breakout***
Maximum load (kips):	***33.4***
Observation	The insert in the top part broke

Figure A7.2 The image of the specimen before failure and after failure.

Appendix A7.3

Sample: FCI 1in. (h_{ef} = 5.51in.) - **03**

Mode of failure: ***Cone breakout***

Maximum load (kips): ***33.2***

Observation -

Figure A7.3 The image of the specimen before failure and after failure.

Appendix B

Pull-out Tension Test

(Edge)

Appendix B1.1

Sample: FCI 1in. (h_{ef} = 5.51in.) - **01**
Mode of failure: ***Splitting + Cone breakout***
Maximum load (kips): ***14.3***
Observation

Figure B1.1 The image of the specimen before failure and after failure.

Appendix B1.2

Sample:	FCI 1in. (h_{ef} = 5.51in.) - **02**
Mode of failure:	***Splitting***
Maximum load (kips):	***14.7***
Observation	-

Figure B1.2 The image of the specimen before failure and after failure.

Appendix B1.3

Sample:	FCI 1in. (h_{ef} = 5.51in.) **- 03**
Mode of failure:	***Splitting***
Maximum load (kips):	***16.4***
Observation	The insert in the top part broke

Figure B1.3 The image of the specimen before failure and after failure.

Appendix B2.1

Sample:	FCI 1in. (h_{ef} = 4.72in.) - **01**
Mode of failure:	***Splitting + Cone breakout***
Maximum load (kips):	***16.03***
Observation	-

Figure B2.1 The image of the specimen before failure and after failure.

Appendix B2.2

Sample: FCI 1in. (h_{ef} = 4.72in.) - **02**

Mode of failure: ***Splitting + Cone breakout***

Maximum load (kips): ***15.13***

Observation -

Figure B2.2 The image of the specimen before failure and after failure.

Appendix B2.3

Sample:	FCI 1in. (h_{ef} = 4.72in.) - **03**
Mode of failure:	***Splitting + Cone breakout***
Maximum load (kips):	***14.87***
Observation	-

Figure B2.3 The image of the specimen before failure and after failure.

Appendix B3.1

Sample: FCI 5/8in. (h_{ef} = 3.37in.) - **01**

Mode of failure: ***Cone breakout***

Maximum load (kips): ***7.94***

Observation -

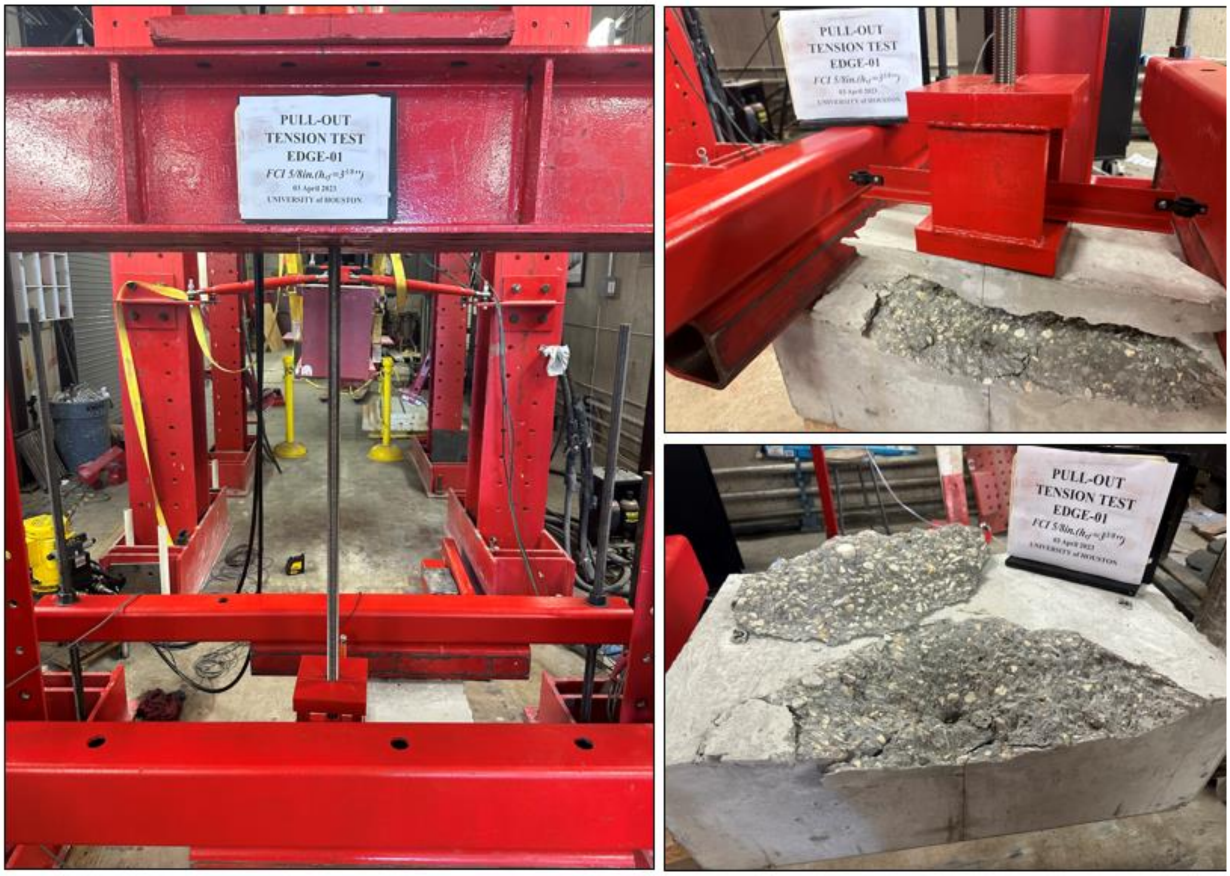

Figure B3.1 The image of the specimen before failure and after failure.

Appendix B3.2

Sample: FCI 5/8in. (h_{ef} = 3.37in.) **- 02**

Mode of failure: ***Cone breakout***

Maximum load (kips): ***8.03***

Observation -

Figure B3.2 The image of the specimen before failure and after failure.

Appendix B3.3

Sample: FCI 5/8in. (h_{ef} = 3.37in.) - **03**

Mode of failure: ***Cone breakout***

Maximum load (kips): ***7.85***

Observation -

Figure B3.3 The image of the specimen before failure and after failure.

Appendix B4.1

Sample: FCI 5/8in. (h_{ef} = 2.97in.) - **01**
Mode of failure: ***Cone breakout***
Maximum load (kips): ***6.78***
Observation -

Figure B4.1 The image of the specimen before failure and after failure.

Appendix B4.2

Sample:	FCI 5/8in. (h_{ef} = 2.97in.) - **02**
Mode of failure:	***Cone breakout***
Maximum load (kips):	***7.13***
Observation	-

Figure B4.2 The image of the specimen before failure and after failure.

Appendix B4.3

Sample: FCI 5/8in. (h_{ef} = 2.97in.) - **03**

Mode of failure: ***Cone breakout***

Maximum load (kips): ***6.40***

Observation -

Figure B4.3 The image of the specimen before failure and after failure.

Appendix B5.1

Sample:	FCI 1/2in. (h_{ef} =3.11in.) - **01**
Mode of failure:	***Cone breakout***
Maximum load (kips):	***7.64***
Observation	- The insert in the bottom part broke

Figure B5.1 The image of the specimen before failure and after failure.

Appendix B5.2

Sample: FCI 1/2in. (h_{ef} =3.11in.) - **02**

Mode of failure: ***Cone breakout***

Maximum load (kips): ***8.23***

Observation
- The insert in the bottom part broke

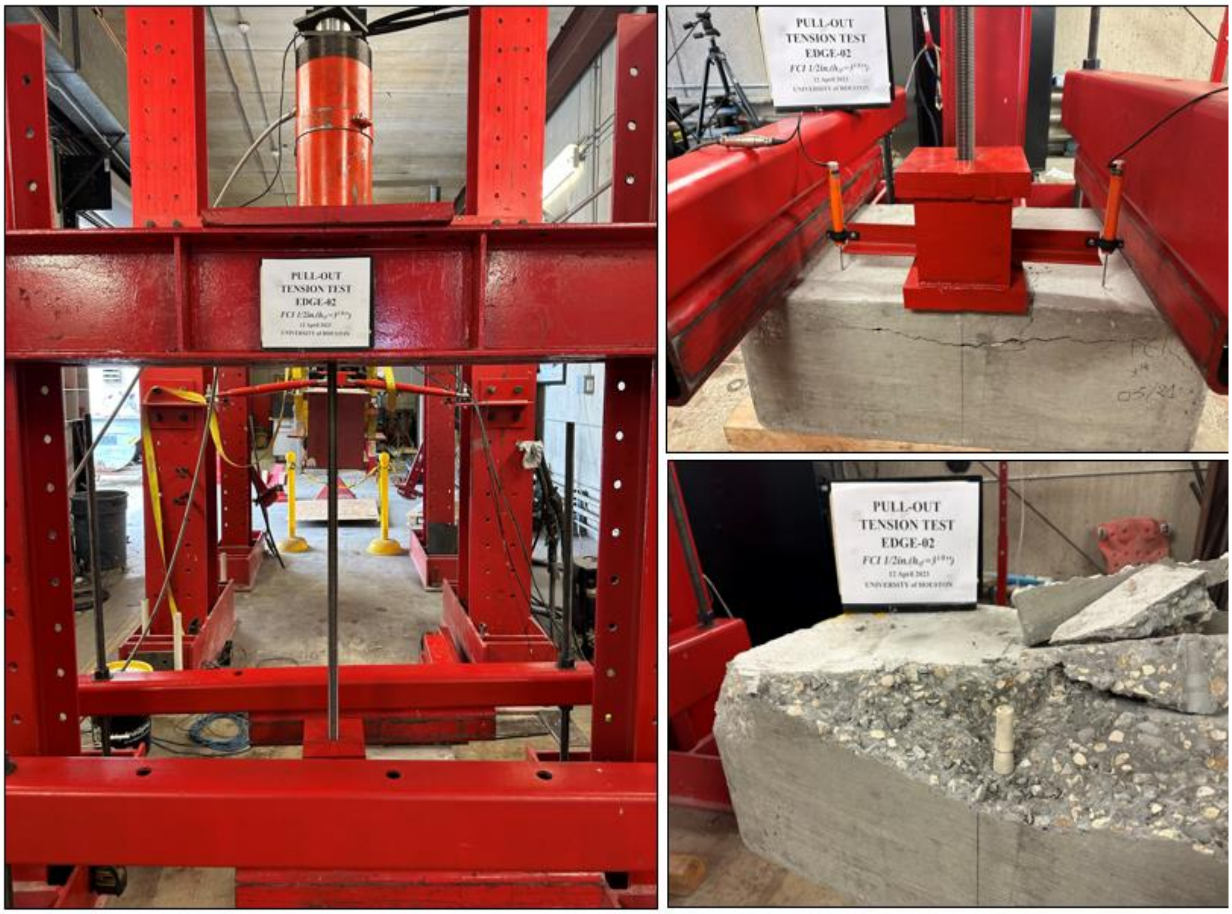

Figure B5.2 The image of the specimen before failure and after failure.

Appendix B5.3

Sample: FCI 1/2in. (h_{ef} =3.11in.) - **03**

Mode of failure: ***Cone breakout***

Maximum load (kips): ***8.97***

Observation - The insert in the bottom part broke

Figure B5.3 The image of the specimen before failure and after failure.

Appendix B6.1

Sample:	FCI 1/2in. (h_{ef} =2.34in.) - **01**
Mode of failure:	***Cone breakout***
Maximum load (kips):	-
Observation	- The insert in the bottom part broke

Figure B6.1 The image of the specimen before failure and after failure.

Appendix B6.2

Sample:	FCI 1/2in. (h_{ef} =2.34in.) - **02**
Mode of failure:	***Cone breakout***
Maximum load (kips):	***5.56***
Observation	-

Figure B6.2 The image of the specimen before failure and after failure.

Appendix B6.3

Sample:	FCI 1/2in. (h_{ef} =2.34in.) **- 03**
Mode of failure:	***Cone breakout***
Maximum load (kips):	***6.31***
Observation	-

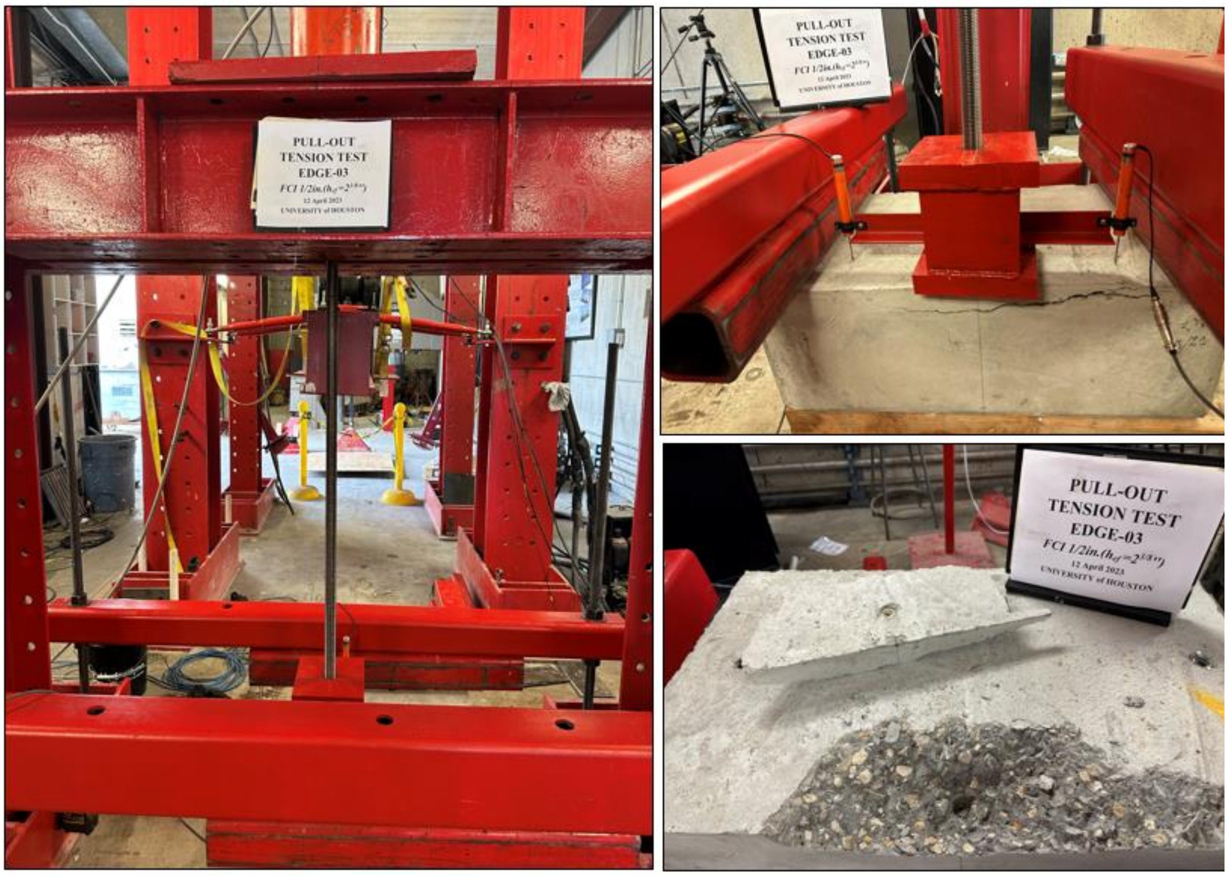

Figure B6.3 The image of the specimen before failure and after failure.

Appendix C

Pull-out Shear Test

(h_a >1.5 C_{a1})

Appendix C1.1

Sample:	FCI 1in. (h_{ef} = 5.51in.) - **01**
Mode of failure:	***Cone breakout + Vertical crack along the specimen depth***
Maximum load (kips):	***17.80***
Observation	- Vertical crack along the specimen depth - FCI failure at the top

Figure C1.1 The image of the specimen before failure and after failure.

Appendix C1.2

Sample:	FCI 1in. (h_{ef} = 5.51in.) - **02**
Mode of failure:	***Cone breakout***
Maximum load (kips):	***17.20***
Observation	- FCI failure at the top

Figure C1.2 The image of the specimen before failure and after failure.

Appendix C1.3

Sample: FCI 1in. (h_{ef} = 5.51in.) - **03**

Mode of failure: ***Cone breakout***

Maximum load (kips): ***16.20***

Observation
- FCI failure at the top

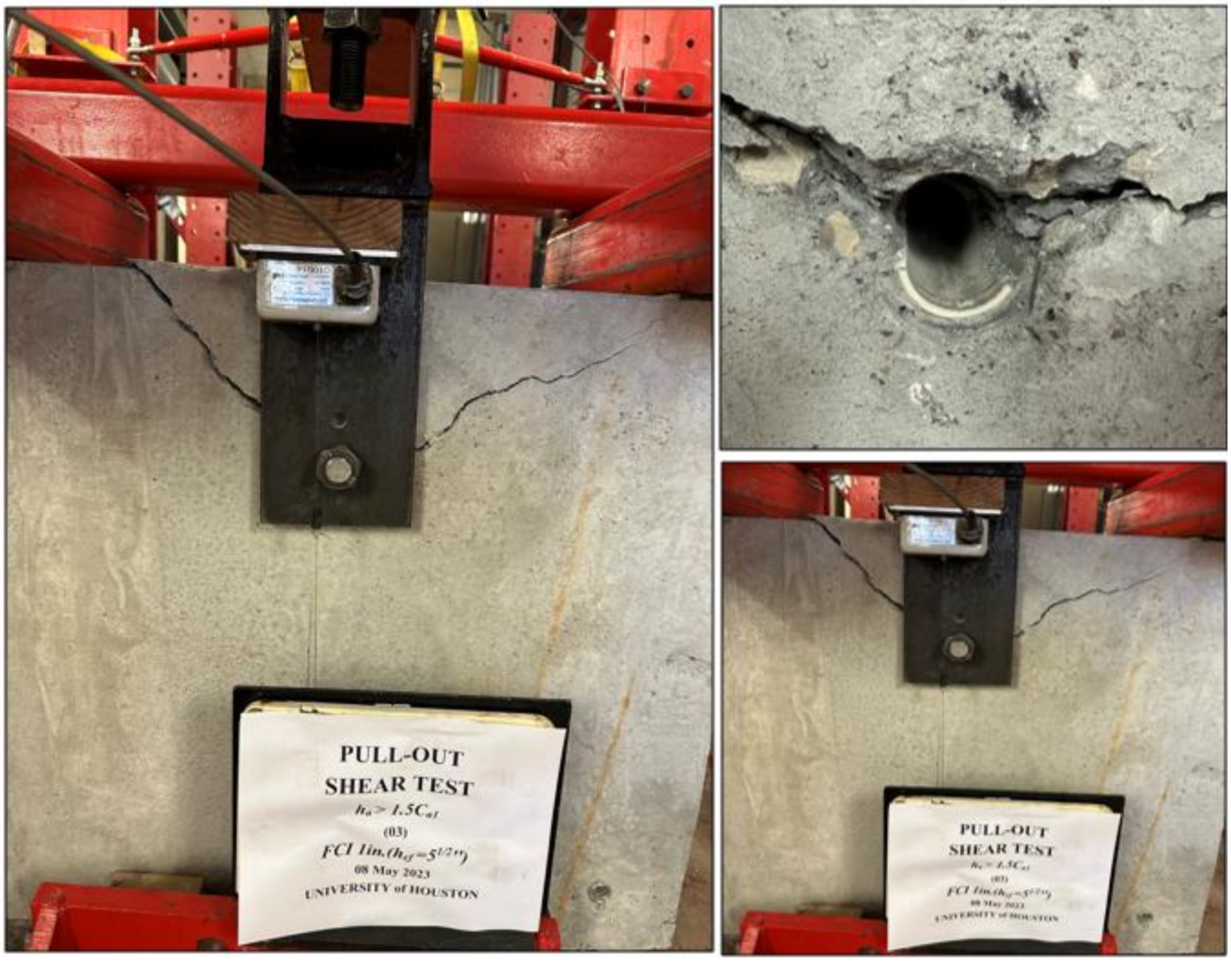

Figure C1.3 The image of the specimen before failure and after failure.

Appendix C2.1

Sample: FCI 1in. (h_{ef} = 4.72 in.) - **01**

Mode of failure: ***Cone breakout + Vertical crack along the specimen depth***

Maximum load (kips): ***17.40***

Observation

- FCI failure at the top
- Vertical crack along the specimen depth

Figure C2.1 The image of the specimen before failure and after failure.

Appendix C2.2

Sample:	FCI 1in. (h_{ef} = 4.72 in.) - **02**
Mode of failure:	***Cone breakout***
Maximum load (kips):	***18.60***
Observation	- FCI failure at the top

Figure C2.2 The image of the specimen before failure and after failure.

Appendix C2.3

Sample: FCI 1in. (h_{ef} = 4.72 in.) - **03**

Mode of failure: ***Cone breakout***

Maximum load (kips): ***16.60***

Observation

- FCI failure at the top

Figure C2.3 The image of the specimen before failure and after failure.

Appendix C3.1

Sample: FCI 5/8in. (h_{ef} = 3.37 in.) **- 01**
Mode of failure: ***Cone breakout***
Maximum load (kips): ***8.10***
Observation
- FCI failure at the top

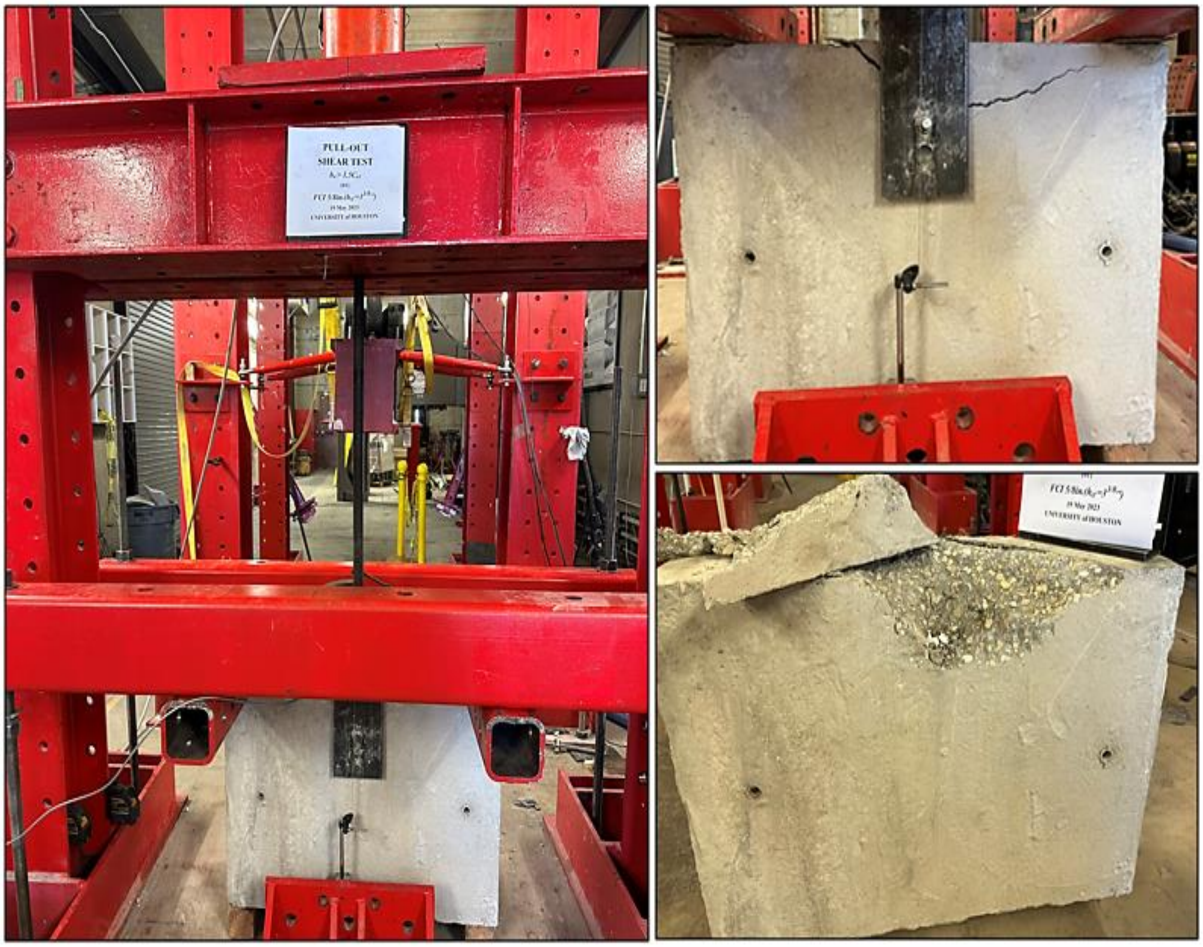

Figure C3.1 The image of the specimen before failure and after failure.

Appendix C3.2

Sample: FCI 5/8in. (h_{ef} = 3.37 in.) **- 02**

Mode of failure: ***Cone breakout***

Maximum load (kips): ***9.20***

Observation
- FCI failure at the top

Figure C3.2 The image of the specimen before failure and after failure.

Appendix C3.3

Sample: FCI 5/8in. (h_{ef} = 3.37 in.) **- 03**

Mode of failure: ***Cone breakout***

Maximum load (kips): ***7.80***

Observation
- FCI failure at the top

Figure C3.3 The image of the specimen before failure and after failure.

Appendix C4.1

Sample: FCI 5/8in. (h_{ef} = 2.97 in.) - **01**

Mode of failure: ***Cone breakout***

Maximum load (kips): ***9.00***

Observation

- FCI failure at the top

Figure C4.1 The image of the specimen before failure and after failure.

Appendix C4.2

Sample: FCI 5/8in. (h_{ef} = 2.97 in.) - **02**

Mode of failure: ***Cone breakout***

Maximum load (kips): ***8.10***

Observation
- FCI failure at the top

Figure C4.2 The image of the specimen before failure and after failure.

Appendix C4.3

Sample:	FCI 5/8in. (h_{ef} = 2.97 in.) - **03**
Mode of failure:	***Cone breakout***
Maximum load (kips):	***8.40***
Observation	- FCI failure at the top

Figure C4.3 The image of the specimen before failure and after failure.

Appendix C5.1

Sample: FCI 1/2in. (h_{ef} = 3.11 in.) - **01**

Mode of failure: ***Cone breakout***

Maximum load (kips): ***8.50***

Observation

- FCI failure at the top

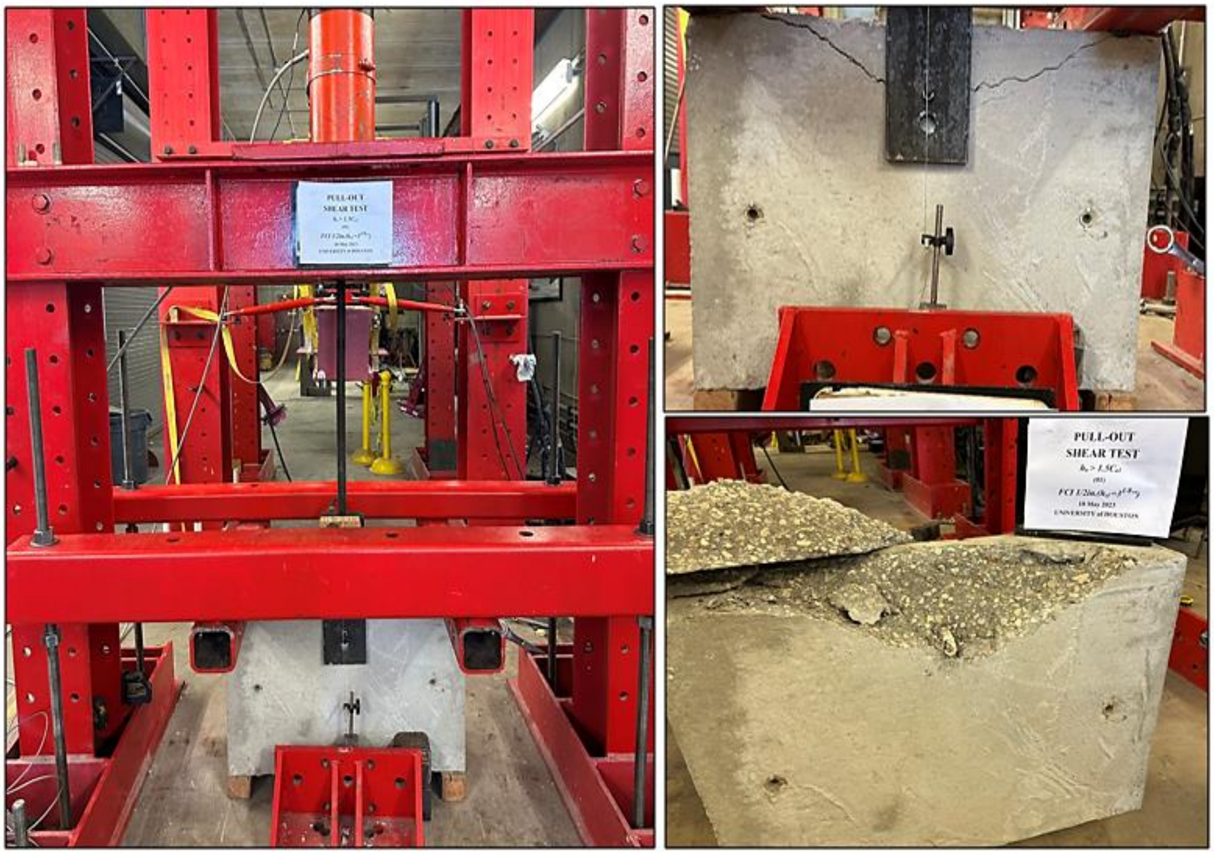

Figure C5.1 The image of the specimen before failure and after failure.

Appendix C5.2

Sample: FCI 1/2in. (h_{ef} = 3.11 in.) - **02**

Mode of failure: ***Cone breakout***

Maximum load (kips): ***8.65***

Observation

- FCI failure at the top

Figure C5.2 The image of the specimen before failure and after failure.

Appendix C5.3

Sample: FCI 1/2in. (h_{ef} = 3.11 in.) - **03**

Mode of failure: ***Cone breakout***

Maximum load (kips): ***8.10***

Observation
- FCI failure at the top

Figure C5.3 The image of the specimen before failure and after failure.

Appendix C6.1

Sample: FCI 1/2in. (h_{ef} = 2.34 in.) - **01**

Mode of failure: ***Cone breakout***

Maximum load (kips): ***7.50***

Observation - FCI failure at the top

Figure C6.1 The image of the specimen before failure and after failure.

Appendix C6.2

Sample: FCI 1/2in. (h_{ef} = 2.34 in.) **- 02**

Mode of failure: ***Cone breakout***

Maximum load (kips): ***8.30***

Observation
- FCI failure at the top

Figure C6.2 The image of the specimen before failure and after failure.

Appendix C6.3

Sample:	FCI 1/2in. (h_{ef} = 2.34 in.) **- 03**
Mode of failure:	***Cone breakout***
Maximum load (kips):	***8.60***
Observation	- FCI failure at the top

Figure C6.3 The image of the specimen before failure and after failure.

Appendix D

Pull-out Shear Test

($h_a < 1.5C_{a1}$)

Appendix D1.1

Sample:	FCI 1in. (h_{ef} = 5.51in.) - **01**
Mode of failure:	***Cone breakout***
Maximum load (kips):	***28.00***
Observation	- FCI failure at the top

Figure D1.1 The image of the specimen before failure and after failure.

Appendix D1.2

Sample: FCI 1in. (h_{ef} = 5.51in.) **- 02**

Mode of failure: ***Cone breakout***

Maximum load (kips): ***29.7***

Observation
- FCI failure at the top

Figure D1.2 The image of the specimen before failure and after failure.

Appendix D1.3

Sample: FCI 1in. (h_{ef} = 5.51in.) **- 03**

Mode of failure: ***Cone breakout***

Maximum load (kips): ***28.50***

Observation

- FCI failure at the top

Figure D1.3 The image of the specimen before failure and after failure.

Appendix D2.1

Sample: FCI 1in. (h_{ef} = 4.72in.) - **01**

Mode of failure: ***Cone breakout***

Maximum load (kips): ***26.10***

Observation

- FCI failure at the top

Figure D2.1 The image of the specimen before failure and after failure.

Appendix D2.2

Sample: FCI 1in. (h_{ef} = 4.72in.) - **02**

Mode of failure: ***Cone breakout***

Maximum load (kips): ***26.80***

Observation
- FCI failure at the top

Figure D2.2 The image of the specimen before failure and after failure.

Appendix D2.3

Sample: FCI 1in. (h_{ef} = 4.72in.) - **03**

Mode of failure: ***Cone breakout***

Maximum load (kips): ***28.40***

Observation

- FCI failure at the top

Figure D2.3 The image of the specimen before failure and after failure.

Appendix D3.1

Sample: FCI 5/8in. (h_{ef} = 3.37in.) - **01**

Mode of failure: ***Cone breakout***

Maximum load (kips): ***14.40***

Observation
- FCI failure at the top

Figure D3.1 The image of the specimen before failure and after failure.

Appendix D3.2

Sample:	FCI 5/8in. (h_{ef} = 3.37in.) - **02**
Mode of failure:	***Cone breakout***
Maximum load (kips):	***13.3***
Observation	- FCI failure at the top

Figure D3.2 The image of the specimen before failure and after failure.

Appendix D3.3

Sample: FCI 5/8in. (h_{ef} = 3.37in.) **- 03**

Mode of failure: ***Cone breakout***

Maximum load (kips): ***13.26***

Observation
- FCI failure at the top
- Vertical crack along the specimen depth

Figure D3.3 The image of the specimen before failure and after failure.

Appendix D4.1

Sample: FCI 5/8in. (h_{ef} = 2.97in.) **- 01**

Mode of failure: ***Cone breakout***

Maximum load (kips): ***13.70***

Observation
- FCI failure at the top

Figure D4.1 The image of the specimen before failure and after failure.

Appendix D4.2

Sample: FCI 5/8in. (h_{ef} = 2.97in.) **- 02**

Mode of failure: ***Cone breakout***

Maximum load (kips): ***12.77***

Observation
- FCI failure at the top

Figure D4.2 The image of the specimen before failure and after failure.

Appendix D4.3

Sample:	FCI 5/8in. (h_{ef} = 2.97in.) **- 03**
Mode of failure:	***Cone breakout***
Maximum load (kips):	***12.63***
Observation	- FCI failure at the top

Figure D4.3 The image of the specimen before failure and after failure.

Appendix D5.1

Sample:	FCI 1/2in. (h_{ef} = 3.11in.) **- 01**
Mode of failure:	***Anchor Failure***
Maximum load (kips):	***10.13***
Observation	- FCI failure at the top

Figure D5.1 The image of the specimen before failure and after failure.

Appendix D5.2

Sample: FCI 1/2in. (h_{ef} = 3.11in.) **- 02**

Mode of failure: ***Anchor Failure***

Maximum load (kips): ***9.2***

Observation
- FCI failure at the top

Figure D5.2 The image of the specimen before failure and after failure.

Appendix D5.3

Sample: FCI 1/2in. (h_{ef} = 3.11in.) **- 03**

Mode of failure: ***Anchor Failure***

Maximum load (kips): ***12.5***

Observation
- FCI failure at the top

Figure D5.3 The image of the specimen before failure and after failure.

Appendix D6.1

Sample: FCI 1/2in. (h_{ef} = 2.34 in.) **- 01**

Mode of failure: ***Anchor Bending***

Maximum load (kips): ***12.00***

Observation
- FCI failure at the top

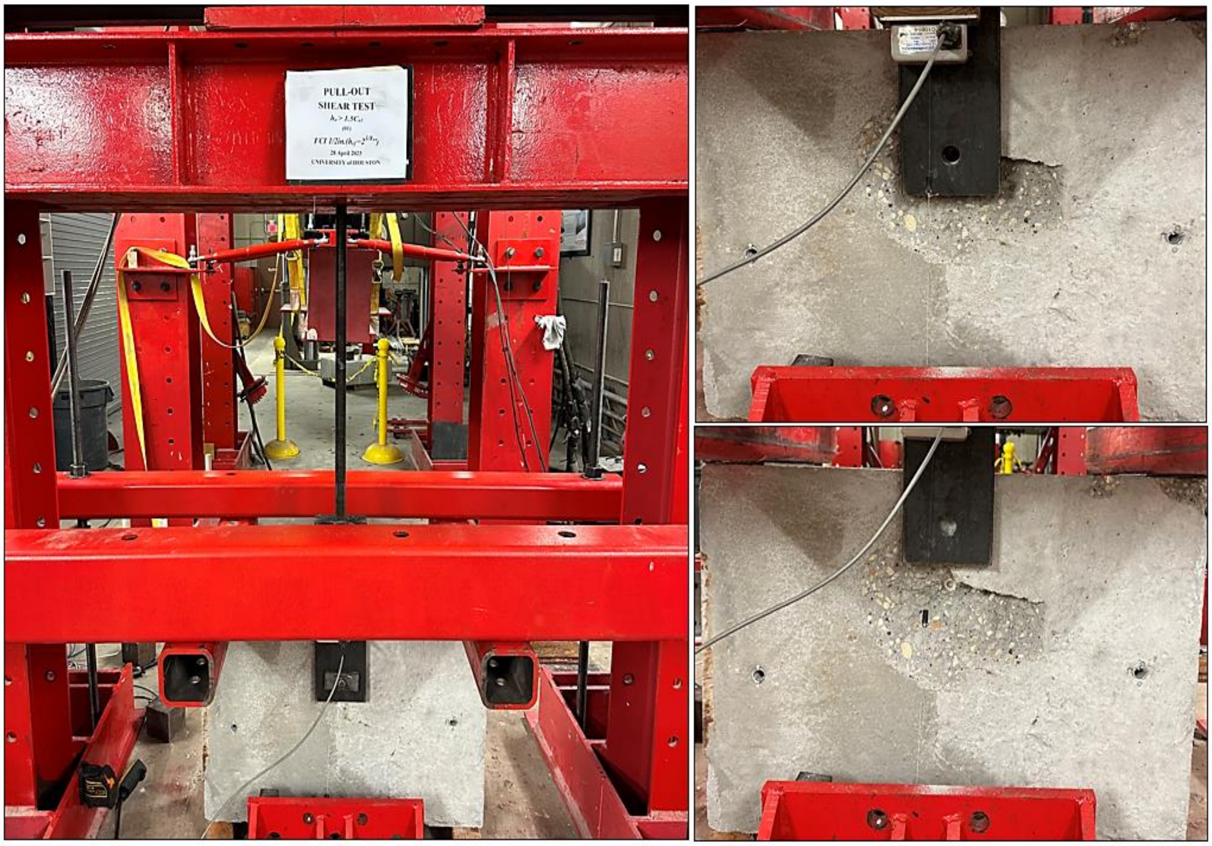

Figure D6.1 The image of the specimen before failure and after failure.

Appendix D6.2

Sample:	FCI 1/2in. (h_{ef} = 2.34 in.) **- 02**
Mode of failure:	***Anchor Bending***
Maximum load (kips):	***12.90***
Observation	- FCI failure at the top

Figure D6.2 The image of the specimen before failure and after failure.

Appendix D6.3

Sample: FCI 1/2in. (h_{ef} = 2.34 in.) - **03**

Mode of failure: ***Cone Breakout Anchor Bending***

Maximum load (kips): ***9.20***

Observation
- FCI failure at the top

Figure D6.3 The image of the specimen before failure and after failure.